

Frequency Dependent Polarization of Repeating Fast Radio Bursts - Implications for Their Origin

Yi Feng,^{1,2,3} Di Li,^{1,2,12*} Yuan-Pei Yang,⁴ Yongkun Zhang,^{1,3} Weiwei Zhu,¹ Bing Zhang,^{5,13}
 Wenbin Lu,⁶ Pei Wang,¹ Shi Dai,⁷ Ryan S. Lynch,⁸ Jumei Yao,⁹ Jinchen Jiang,^{1,10}
 Jiarui Niu,^{1,3} Dejiang Zhou,^{1,3} Heng Xu,^{1,10} Chenchen Miao,^{1,3} Chenhui Niu,¹
 Lingqi Meng,^{1,3} Lei Qian,¹ Chao-Wei Tsai,¹ Bojun Wang,^{1,10} Mengyao Xue,¹
 Youling Yue,¹ Mao Yuan,^{1,3} Songbo Zhang,¹¹ Lei Zhang¹

¹National Astronomical Observatories, Chinese Academy of Sciences, Beijing 100101, China

²Zhejiang Lab, Hangzhou, Zhejiang 311121, China

³University of Chinese Academy of Sciences, Beijing 100049, China

⁴South-Western Institute for Astronomy Research, Yunnan University, Kunming, Yunnan, China

⁵ Department of Physics and Astronomy, University of Nevada, Las Vegas, NV 89154, USA

⁶ Department of Astrophysical Sciences, Princeton University, Princeton, NJ 08544, USA

⁷School of Science, Western Sydney University, Penrith NSW 2751, Australia

⁸Green Bank Observatory, Green Bank, WV, 24401, USA

⁹Xinjiang Astronomical Observatory, Chinese Academy of Sciences, Urumqi, Xinjiang 830011, China

¹⁰School of Physics, Peking University, Beijing 100871

¹¹Purple Mountain Observatory, Chinese Academy of Sciences, Nanjing 210023, China

¹²National Astronomical Observatories, Chinese Academy of Sciences-University of KwaZulu-Natal
 Computational Astrophysics Centre, University of KwaZulu-Natal, Durban 4000, South Africa

¹³ Nevada Center for Astrophysics, University of Nevada, Las Vegas, NV 89154, USA

* Corresponding author. E-mail:dili@nao.cas.cn

The polarization of fast radio bursts (FRBs), bright astronomical transients, contains crucial information about their environments. We report polarization measurements of five repeating FRBs, the abundant signals of which enable wide-band observations with two telescopes. A clear trend of lower polar-

ization at lower frequencies was found, which can be well characterized by a single parameter rotation-measure-scatter (σ_{RM}) and modeled by multi-path scatter. Sources with higher σ_{RM} have higher RM magnitude and scattering timescales. The two sources with the most substantial σ_{RM} , FRB 20121102A and FRB 20190520B, are associated with a compact persistent radio source. These properties indicate a complex environment near the repeating FRBs, such as a supernova remnant or a pulsar wind nebula, consistent with their arising from young populations.

Fast radio bursts (FRBs) are the brightest millisecond-duration-astronomical transients in radio bands (1). Some FRBs are known to repeat, such as FRB 20121102A (2), but it remains unclear whether repeating fast radio bursts (hereafter repeaters) are ubiquitous or peculiar sources. Whether all FRBs repeat on some time scale, or if repeaters form a separate population from single-burst sources, has implications for the energy source (3), host environments (4), luminosity function (5), apparent and intrinsic event rates (6), and predicted survey yields (7).

Information about the FRB hosts and environments could be obtained from their polarization. Faraday rotation is a phenomenon where the polarization position angle of linearly polarized radiation propagating through a magneto-ionic medium is rotated as a function of frequency, quantified by the Rotation Measure (RM), which carries information about the local environment and the intervening medium. The substantial and time-varying RM of FRB 20121102A has been interpreted as due to a dynamic magneto-ionic environment (8), such as an expanding supernova remnant or a pulsar wind nebula (9, 10). The polarization position angle and fraction of linear/circular polarization could constrain the emission mechanisms (11, 12). For example, a constant polarization position angle across a burst is consistent with either a far-away model invoking a relativistic shock or emission from the outer magnetosphere of a neutron star (3). Alternatively, the varying polarization angle observed in the repeater FRB 20180301A has been

interpreted as originating within the magnetosphere of a magnetar (a highly magnetized neutron star) (*13*).

We analyze the polarization properties of 21 FRB sources, 9 of which have been confirmed to repeat. We observed five of them, FRB 20121102A, FRB 20190520B, FRB 20190303A, FRB 20190417A, and FRB 20201124A using the Five-hundred-meter Aperture Spherical radio Telescope (FAST) and the Robert C. Byrd Green Bank Telescope (GBT). The other 16 sources are taken from the literature (listed in Table S1). Our goal is to examine their RM, linear polarization fraction and its dependence on frequency.

The repeater FRB 20121102A has been precisely localized to a dwarf galaxy (*2, 14*). It has a bimodal burst energy distribution with 1652 independent bursts detected in 59.5 hours spanning 62 days (*15*). Using the same dataset, we searched RM in each of the 1652 bursts and detected no linear polarization setting a 6% upper limit on the degree of linear polarization at 1.0-1.5 GHz (*16*). For comparison, previous observations showed almost 100% linear polarization at 3-8 GHz (*8*).

FRB 20190520B is another repeater localized to a persistent radio source (PRS) in another dwarf galaxy (*17, 18*). An RM search for the 75 bursts presented in Ref. 18 resulted in no detection, with an upper limit of 20% on the degree of linear polarization at 1.0-1.5 GHz (*16*). Our follow-up observations with the GBT detected three bursts from 4-8 GHz band with an average RM of 2759 rad m^{-2} (*16*). Representative polarization pulse profiles and dynamic spectra of this source are shown in Figure 1C.

FRBs 20190303A, 20190417A, and 20201124A were discovered at 400–800 MHz (*19, 20*). We followed up these sources with the FAST 19-beam system at 1.0-1.5 GHz. From FRB 20190303A, 3 bursts were detected with an average RM of -411 rad m^{-2} , which help localize the source to (Right Ascension–RA, Declination–Dec) = $(13^{\text{h}}51^{\text{m}}58^{\text{s}}, +48^{\circ}07'20'')$ (J2000) with a $2.6'$ error circle (*16*). Compared with the earlier lower-frequency measurements (*19*),

the RM has changed about 100 rad/m^2 over 1.5-year timespan. In contrast to the earlier low linear polarization (19), the bursts detected with FAST are nearly 100% linearly polarized. From FRB 20190417A, we detected 23 bursts, 5 of which have measurable polarization with an average RM of 4681 rad m^{-2} . The estimated position of FRB 20190417A is (RA, DEC) = ($19^{\text{h}}39^{\text{m}}22^{\text{s}}$, $+59^{\circ}18'58''$) (J2000) with an error circle of $2.6'$ (16). FAST follow-up observations of FRB 20201124A resulted in a large sample bursts, of which 11 were bright enough to be used in our analysis (16). We also detected 9 polarized bursts with the GBT at 720–920 MHz, with an average RM of -684 rad m^{-2} . Both FRB 20190417A and FRB 20201124A have higher linear polarization at higher frequencies. The average RMs of each FRB are listed in Table S2. The time of arrival (ToA), the central frequency of the burst emission (weighted by the burst signal-to-noise ratio as a function of frequency), the intra-channel depolarization f_{depol} (see below and Eq. 1), RM, and degree of de-biased (16) linear and circular polarization of each pulse are listed in Table S3. Representative polarization pulse profiles and their dynamic spectra are shown in Figure 1 (16).

The observations of these four sources all indicate decreasing linear polarization with decreasing frequencies. To explain this behaviour, we consider three effects: i) intrinsic frequency evolution of the linear polarization, ii) intra-channel depolarization, and iii) RM scatter.

Intrinsic frequency evolution of linear polarization is already known for pulsars (21). The polarization tends to decrease from lower to higher frequencies, which has been attributed to emission from different heights in the pulsar magnetospheres (22). This is the opposite trend to the one we find for repeating FRBs, so a direct analogy is not supported. Given the lack of understanding of FRB origin(s), our results cannot rule out other scenarios involving pulsar-magnetosphere-like environments.

The alternative intra-channel depolarization f_{depol} , the fractional reduction in the linear po-

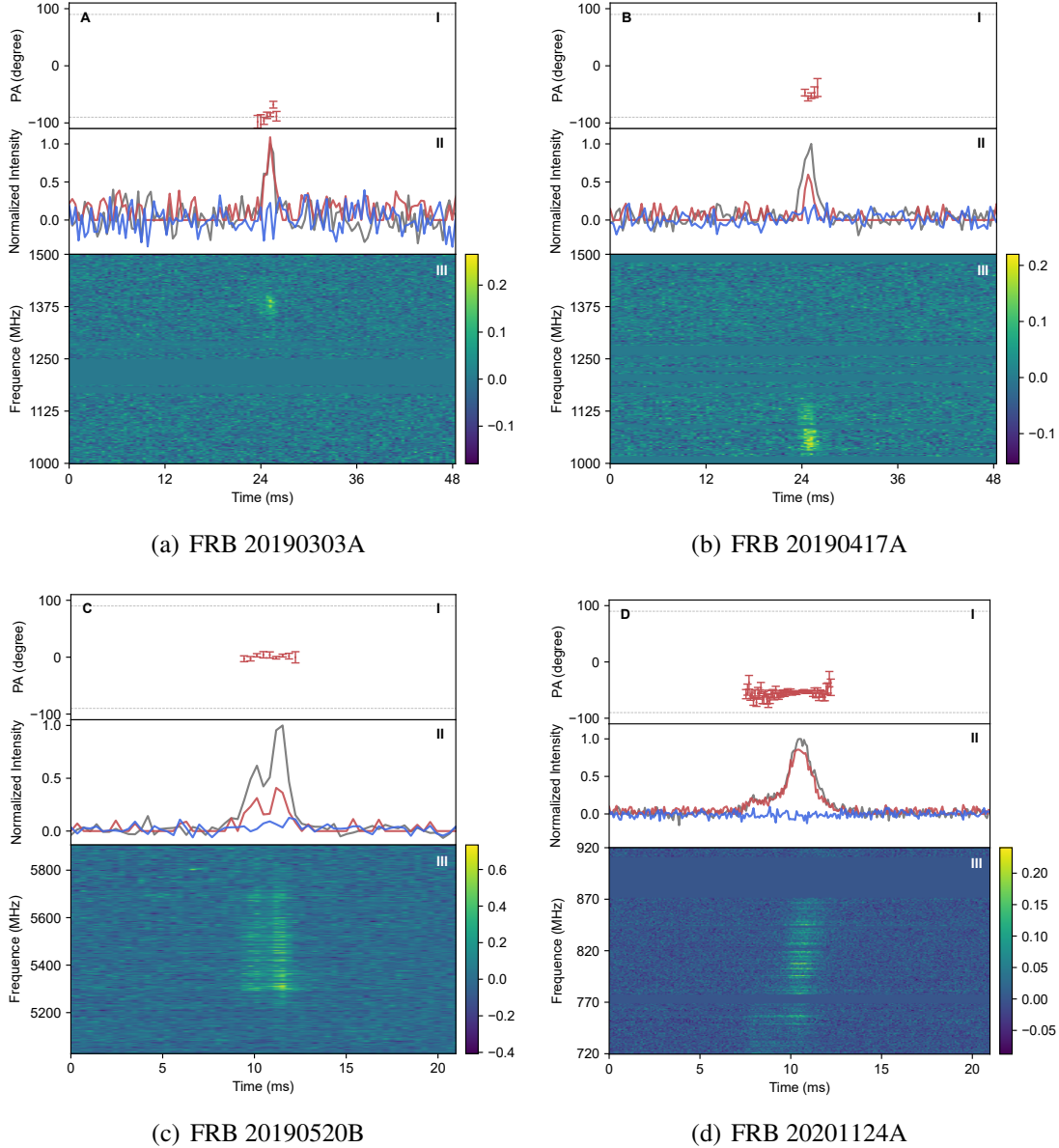


Figure 1: **Polarization position angle and intensity profiles with dynamic spectra for four repeating FRBs.** In each panel, sub-panel I shows the polarization position angles with gray dashed lines indicating $\pm 90^\circ$; sub-panel II shows the polarization pulse profiles with lines indicating total intensity (black, normalized to a peak value of 1.0), linear polarization (red) and circular polarization (blue); sub-panel III shows the dynamic spectra.

larization amplitude, is defined as:

$$f_{\text{depol}} \equiv 1 - \frac{\sin(\Delta\theta)}{\Delta\theta}, \quad (1)$$

where $\Delta\theta$ is the intra-channel polarization position angle rotation. $\Delta\theta$ is defined as $\Delta\theta \equiv \frac{2\text{RM}_{\text{obs}}c^2\Delta\nu}{\nu_c^3}$, where RM_{obs} is the observed rotation measure, c is the speed of light, $\Delta\nu$ is the channel frequency width, and ν_c is the central channel observing frequency. For repeaters, the measured RMs are too small for explaining the depolarization through this effect (f_{depol} listed in Table S1 and Table S3). We infer that intra-channel depolarization is unlikely to be a major cause of depolarization for repeating FRBs.

We next examine RM scattering, the dispersion of RM about the apparent mean for each source (23). RM scattering can be caused by multi-path transmission of signals in an inhomogeneous magneto-ionic environment. If the scattering is large enough, it can become substantial enough to depolarize the pulses, analogous to pulsar pulses passing through a stellar wind (24, 25). We parametrize the depolarization due to RM scattering as (23):

$$f_{\text{RM scattering}} \equiv 1 - \exp(-2\lambda^4\sigma_{\text{RM}}^2), \quad (2)$$

where $f_{\text{RM scattering}}$ is the fractional reduction in the linear polarization amplitude, σ_{RM} is the standard deviation of the RM and λ is the wavelength.

Depolarization at lower frequencies, consistent with irregular RM variations, has been seen in a few pulsars with scatter broadening. For example, the variable degree of linear polarization observed in the pulsar PSR J0742–2822 between 200 MHz and 1 GHz can be described by Eq. 2 with $\sigma_{\text{RM}} = 0.13 \text{ rad/m}^2$ (26).

Complex magneto-ionic environments have previously been inferred from observations for some repeaters (8, 13). We also expect RM scatter for FRBs in such environments. In Figure 2, we show the degree of linear polarization versus frequency for each source individually. Frequency evolution can be seen for all sources, but the depolarization occurs at different

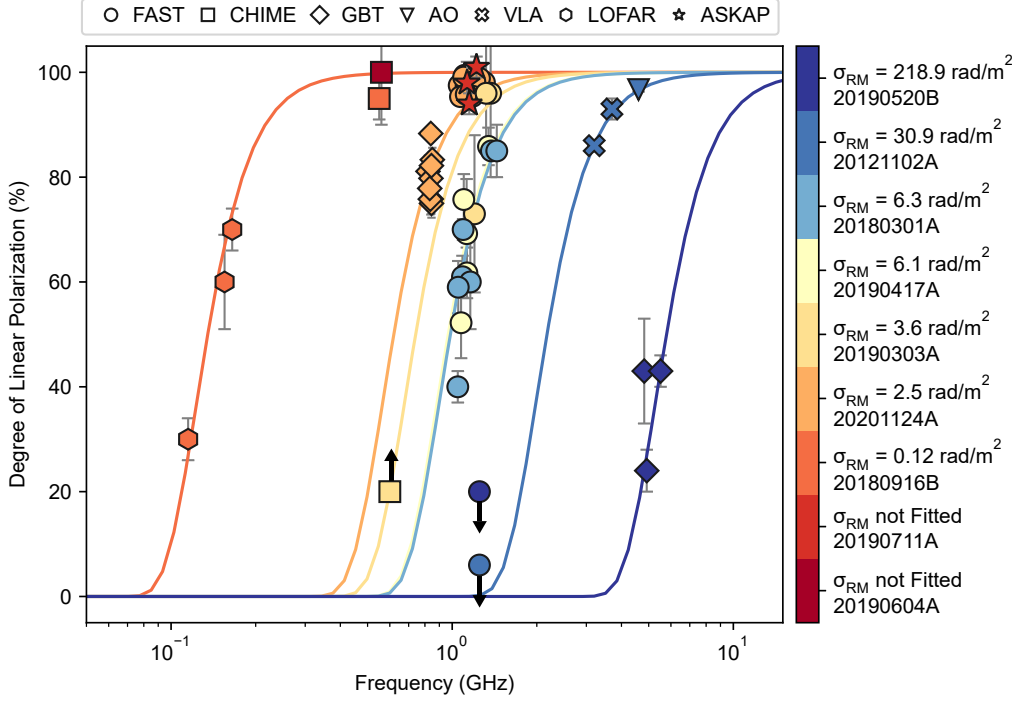


Figure 2: **The degree of linear polarization for FRB sources is consistent with RM scattering.** Data points with 1σ error bars indicate the degree of linear polarization as a function of frequency for each FRB. The colored lines are models of emission that is intrinsically 100% linearly polarized then depolarized by various σ_{RM} levels (Equation 2), fitted to each FRB separately. Arrows indicate 95% upper and lower limits. All the bursts in the sample are consistent with the RM scattering models. Data values and sources are listed in Tables S1 and S3, and the model σ_{RM} values in Table S2. CHIME, AO, VLA, LOFAR and ASKAP at the top represents Canadian Hydrogen Intensity Mapping Experiment, Arecibo Observatory, Karl G. Jansky Very Large Array, Low-Frequency Array and Australian Square Kilometre Array Pathfinder, respectively.

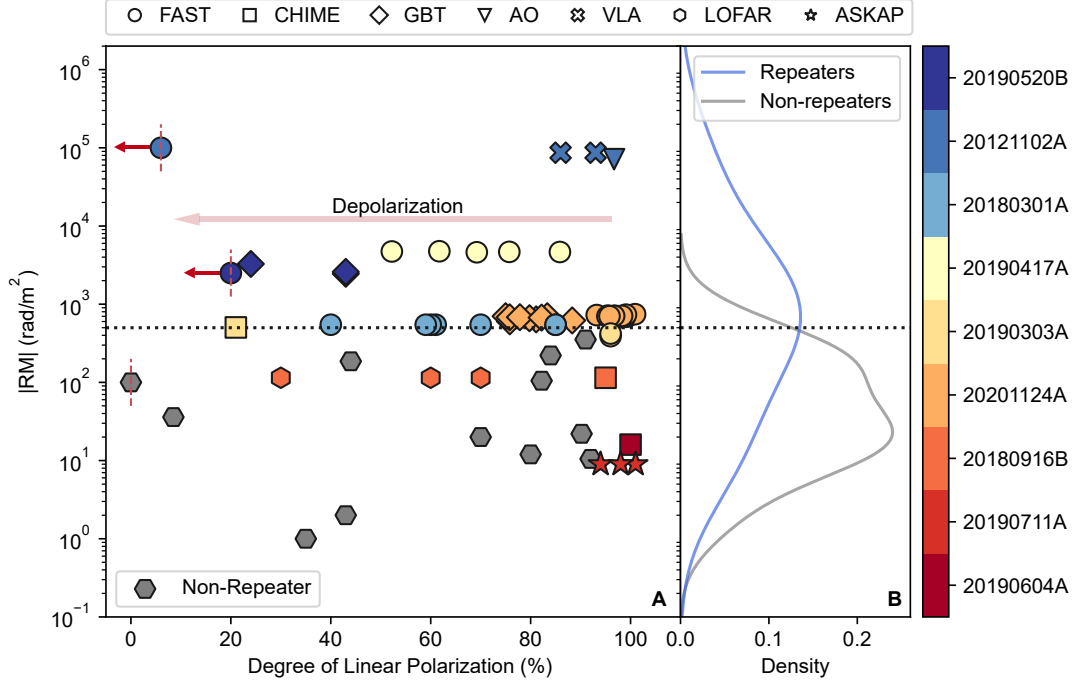


Figure 3: **The relation between RM and degree of linear polarization for repeating and non-repeating FRBs.** The vertical dashed red lines indicate that the respective RM was not detected in L-band. We thus choose nominal values that are either representative or measured at higher frequencies, i.e. 100 rad m^{-2} for FRB 20140514A, 3000 rad m^{-2} for FRB 20190520B and 10^5 rad m^{-2} for FRB 20121102A. The red arrows are 95% upper limits on the linear polarization. The horizontal dotted black line indicates $|\text{RM}| = 500 \text{ rad/m}^2$, which lies above all the non-repeaters. The blue and gray profiles in the panel B are the Kernel Density Estimation (KDE) of the repeaters' RMs and non-repeaters' RMs. The p-value from Kolmogorov-Smirnov test of the repeaters' RM and non-repeaters' RM is 0.02. The acronyms of telescopes at the top are the same as those in Figure 2.

bands. FRB 20180916B is depolarized below 200 MHz (27), while FRB 20121102A (28) is depolarized at frequencies lower than 3.5 GHz. We fitted the data for each repeater using the model in Equation 2, with a different σ_{RM} for each source (16). For the sources depolarized at lower frequencies (<200 MHz), such as FRB 20180916B, we derive $\sigma_{\text{RM}} \sim 0.1 \text{ rad/m}^2$ (Table S2). Such a small scatter is consistent with the environment being less turbulent, dense, and/or magnetized than that of other FRBs, as might be expected for an old stellar population (27). We find $\sigma_{\text{RM}} \sim 2.5 \text{ rad/m}^2$ for FRB 20201124A, $\sigma_{\text{RM}} \sim 3.6 \text{ rad/m}^2$ for FRB 20190303A, $\sigma_{\text{RM}} \sim 6.1 \text{ rad/m}^2$ for FRB 20190417A, $\sigma_{\text{RM}} \sim 6.3 \text{ rad/m}^2$ for FRB 20180301A and $\sigma_{\text{RM}} \sim 30.9 \text{ rad/m}^2$ for FRB 20121102A (Table S2). The RM scatter of 30.9 rad/m^2 is consistent with FRB 20121102A originating in a younger stellar population (28) that produced an inhomogeneous magneto-ionic environment. For the repeater FRB 20190520B, which depolarizes at frequencies higher than 1 GHz, we derive $\sigma_{\text{RM}} \sim 218.9 \text{ rad/m}^2$. The observations are consistent with repeating bursts being intrinsically nearly 100% linearly polarized, then being depolarized through transmission processes, which can be characterized by the RM scatter parameter σ_{RM} . The same environment that gives rise to large σ_{RM} could also cause Faraday conversion wherein linearly polarised light is converted to circularly polarised light, potentially explaining the circular polarization observed in some FRBs (29). We interpret the σ_{RM} values derived from our analysis as a measure of the complexity level of the magneto-ionic environments hosting active repeaters, with larger σ_{RM} values being possibly associated with younger populations.

Figure 3 shows the relation between RM and linear polarization for repeating and non-repeating FRBs in our sample with polarization measurements. A Kolmogorov-Smirnov test between the repeaters and non-repeaters finds the RM distributions differ, indicating they may reside in different environments. We caution that the intra-channel depolarization may introduce a selection bias if the non-repeaters have systematically larger RMs, because discovery searches tend to use coarser filter banks than follow-up observations.

If σ_{RM} is due to multi-path propagation effect in individual FRB bursts, we would expect the same effect to produce a temporal scattering in the pulse profile. In Figure 4, we show RM scatter and scattering timescales, which are listed in Table S2, for our repeater sample. The two are positively correlated. This is consistent with the hypothesis that RM scatter and pulse scattering originate from a single plasma screen, such as a supernova remnant or pulsar wind nebula (30). In Figure 4, σ_{RM} and $|\text{RM}|$ are shown to be correlated positively, which, in the context of our multi-path-scattering model, indicate an environment, where a stronger magnetic field strength B tend to have a larger fluctuation in B .

Only two FRBs FRB 20190520B and FRB 20121102A, are known to have associated compact PRSs (4, 18). We find that these two repeaters have the largest σ_{RM} . The combination of large RM (dense) and strong B field (magnetized) tend to produce large σ_{RM} . A denser and more magnetized environment likely also produces stronger synchrotron radiation from the nebula, resulting in a PRS (31), consistent with the multi-path-scattering picture. Repeaters with large observed σ_{RM} could be more affected by turbulence, resulting in large fluctuations of electron density and magnetic field, which may explain the diversity among repeaters (30).

In summary, σ_{RM} can be used to quantify the complexity of the magnetized environments, which seem to be commonly associated with repeating FRBs. The more substantial the value of σ_{RM} possibly indicates the source being younger.

References

1. D. R. Lorimer, M. Bailes, M. A. McLaughlin, D. J. Narkevic, and F. Crawford, A Bright Millisecond Radio Burst of Extragalactic Origin, *Science* **318**, 777. (2007). 10.1126/science.1147532
2. L. G. Spitler, P. Scholz, J. W. T. Hessels, S. Bogdanov, A. Brazier, F. Camilo, S. Chatterjee,

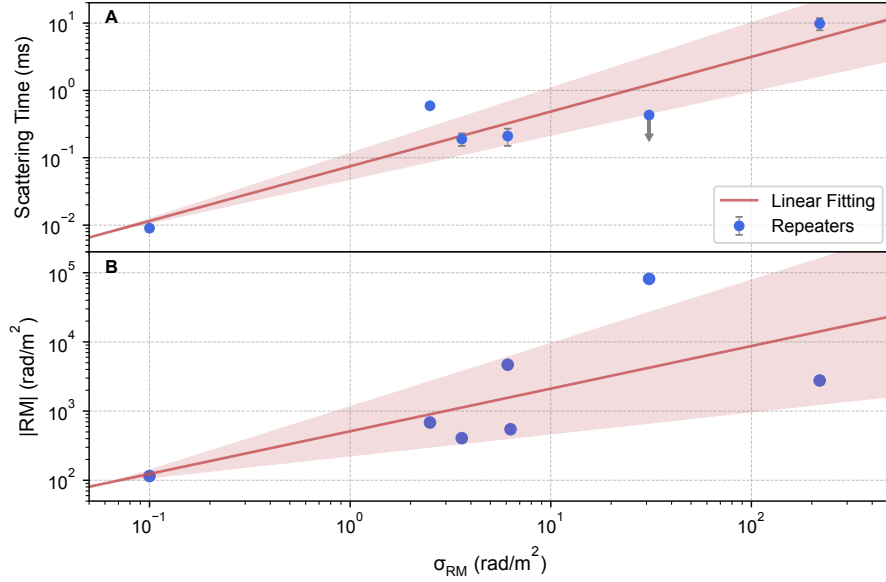


Figure 4: **Correlations between σ_{RM} , scattering time τ_{sca} and rotation measure magnitude $|\text{RM}|$ for repeating FRBs.** Panel A: The relation between σ_{RM} and the scattering timescale scaled to 1300 MHz (16) for repeaters with σ_{RM} measurements. The data used are listed in Table S2. FRB 20121102A is an upper limit (gray arrow). The Pearson product-moment correlation coefficient of $\log \tau_{\text{sca}}$ and $\log \sigma_{\text{RM}}$ is 0.47. Fitting the data with a linear model (red line) gives a slope of 0.81 ± 0.16 . Panel B: The relation between σ_{RM} and $|\text{RM}|$ for the same sample of repeaters. The Pearson product-moment correlation coefficient of $\log |\text{RM}|$ and $\log \sigma_{\text{RM}}$ is 0.68. Fitting the data with a linear model (red line) gives a slope of 0.62 ± 0.30 . All quantities are measured in the observer’s frame. The 1σ uncertainties on σ_{RM} and $|\text{RM}|$ are smaller than the symbol size.

- J. M. Cordes, F. Crawford, J. Deneva, R. D. Ferdman, P. C. C. Freire, V. M. Kaspi, P. Lazarus, R. Lynch, E. C. Madsen, M. A. McLaughlin, C. Patel, S. M. Ransom, A. Seymour, I. H. Stairs, B. W. Stappers, J. van Leeuwen, and W. W. Zhu, A repeating fast radio burst, *Nature* **531**, 202-205. (2016). 10.1038/nature17168
3. B. Zhang, The physical mechanisms of fast radio bursts, *Nature* **587**, 45-53. (2020). 10.1038/s41586-020-2828-1
 4. B. Marcote, Z. Paragi, J. W. T. Hessels, A. Keimpema, H. J. van Langevelde, Y. Huang, C. G. Bassa, S. Bogdanov, G. C. Bower, S. Burke-Spolaor, B. J. Butler, R. M. Campbell, S. Chatterjee, J. M. Cordes, P. Demorest, M. A. Garrett, T. Ghosh, V. M. Kaspi, C. J. Law, T. J. W. Lazio, M. A. McLaughlin, S. M. Ransom, C. J. Salter, P. Scholz, A. Seymour, A. Siemion, L. G. Spitler, S. P. Tendulkar, and R. S. Wharton, The Repeating Fast Radio Burst FRB 121102 as Seen on Milliarcsecond Angular Scales, *The Astrophysical Journal* **834**, L8. (2017). 10.3847/2041-8213/834/2/L8
 5. R. Luo, K. Lee, D. R. Lorimer, and B. Zhang, On the normalized FRB luminosity function, *Monthly Notices of the Royal Astronomical Society* **481**, 2320-2337. (2018). 10.1093/mnras/sty2364
 6. D. W. Gardenier, J. van Leeuwen, L. Connor, and E. Petroff, Synthesising the intrinsic FRB population using frbpoppy, *Astronomy and Astrophysics* **632**, A125. (2019). 10.1051/0004-6361/201936404
 7. J.-P. Macquart and R. D. Ekers, Fast radio burst event rate counts - I. Interpreting the observations, *Monthly Notices of the Royal Astronomical Society* **474**, 1900-1908. (2018). 10.1093/mnras/stx2825

8. D. Michilli, A. Seymour, J. W. T. Hessels, L. G. Spitler, V. Gajjar, A. M. Archibald, G. C. Bower, S. Chatterjee, J. M. Cordes, K. Gourdji, G. H. Heald, V. M. Kaspi, C. J. Law, C. Sobey, E. A. K. Adams, C. G. Bassa, S. Bogdanov, C. Brinkman, P. Demorest, F. Fernandez, G. Hellbourg, T. J. W. Lazio, R. S. Lynch, N. Maddox, B. Marcote, M. A. McLaughlin, Z. Paragi, S. M. Ransom, P. Scholz, A. P. V. Siemion, S. P. Tendulkar, P. van Rooy, R. S. Wharton, and D. Whitlow, An extreme magneto-ionic environment associated with the fast radio burst source FRB 121102, *Nature* **553**, 182-185. (2018). 10.1038/nature25149
9. A. L. Piro and B. M. Gaensler, The Dispersion and Rotation Measure of Supernova Remnants and Magnetized Stellar Winds: Application to Fast Radio Bursts, *The Astrophysical Journal* **861**, 150. (2018). 10.3847/1538-4357/aac9bc
10. B. Margalit and B. D. Metzger, A Concordance Picture of FRB 121102 as a Flaring Magnetar Embedded in a Magnetized Ion-Electron Wind Nebula, *The Astrophysical Journal* **868**, L4. (2018). 10.3847/2041-8213/aaedad
11. W. Lu, P. Kumar, and R. Narayan, Fast radio burst source properties from polarization measurements, *Monthly Notices of the Royal Astronomical Society* **483**, 359-369. (2019). 10.1093/mnras/sty2829
12. S. Dai, J. Lu, C. Wang, W.-Y. Wang, R. Xu, Y. Yang, S. Zhang, G. Hobbs, D. Li, R. Luo, M. Filipovic, and J. Jiang, On the Circular Polarization of Repeating Fast Radio Bursts, *The Astrophysical Journal* **920**, 46. (2021). 10.3847/1538-4357/ac193d
13. R. Luo, B. J. Wang, Y. P. Men, C. F. Zhang, J. C. Jiang, H. Xu, W. Y. Wang, K. J. Lee, J. L. Han, B. Zhang, R. N. Caballero, M. Z. Chen, X. L. Chen, H. Q. Gan, Y. J. Guo, L. F. Hao, Y. X. Huang, P. Jiang, H. Li, J. Li, Z. X. Li, J. T. Luo, J. Pan, X. Pei, L. Qian, J. H. Sun, M. Wang, N. Wang, Z. G. Wen, R. X. Xu, Y. H. Xu, J. Yan, W. M. Yan, D. J. Yu,

- J. P. Yuan, S. B. Zhang, and Y. Zhu, Diverse polarization angle swings from a repeating fast radio burst source, *Nature* **586**, 693-696. (2020). 10.1038/s41586-020-2827-2
14. S. Chatterjee, C. J. Law, R. S. Wharton, S. Burke-Spolaor, J. W. T. Hessels, G. C. Bower, J. M. Cordes, S. P. Tendulkar, C. G. Bassa, P. Demorest, B. J. Butler, A. Seymour, P. Scholz, M. W. Abruzzo, S. Bogdanov, V. M. Kaspi, A. Keimpema, T. J. W. Lazio, B. Marcote, M. A. McLaughlin, Z. Paragi, S. M. Ransom, M. Rupen, L. G. Spitler, and H. J. van Langevelde, A direct localization of a fast radio burst and its host, *Nature* **541**, 58-61. (2017). 10.1038/nature20797
 15. D. Li, P. Wang, W. W. Zhu, B. Zhang, X. X. Zhang, R. Duan, Y. K. Zhang, Y. Feng, N. Y. Tang, S. Chatterjee, J. M. Cordes, M. Cruces, S. Dai, V. Gajjar, G. Hobbs, C. Jin, M. Kramer, D. R. Lorimer, C. C. Miao, C. H. Niu, J. R. Niu, Z. C. Pan, L. Qian, L. Spitler, D. Werthimer, G. Q. Zhang, F. Y. Wang, X. Y. Xie, Y. L. Yue, L. Zhang, Q. J. Zhi, Y. Zhu, A bimodal burst energy distribution of a repeating fast radio burst source, *Nature*. **598**, 267–271 (2021). 10.1038/s41586-021-03878-5
 16. The observations and data analysis are described in Materials and Methods.
 17. D. Li, P. Wang, L. Qian, M. Krco, P. Jiang, Y. Yue, C. Jin, Y. Zhu, Z. Pan, R. Nan, and A. Dunning, FAST in Space: Considerations for a Multibeam, Multipurpose Survey Using China’s 500-m Aperture Spherical Radio Telescope (FAST), *IEEE Microwave Magazine* **19**, 112-119. (2018). 10.1109/MMM.2018.2802178
 18. C.-H. Niu, K. Aggarwal, D. Li, X. Zhang, S. Chatterjee, C.-W. Tsai, W. Yu, C. J. Law, S. Burke-Spolaor, J. M. Cordes, Y.-K. Zhang, S. Ocker, J.-M. Yao, P. Wang, Y. Feng, Y. Niino, C. Bochenek, M. Cruces, L. Connor, J.-A. Jiang, S. Dai, R. Luo, G.-D. Li, C.-C. Miao, J.-R. Niu, R. Anna-Thomas, J. Sydnor, D. Stern, W.-Y. Wang, M. Yuan, Y.-L. Yue,

- D.-J. Zhou, Z. Yan, W.-W. Zhu, B. Zhang, A repeating FRB in a dense environment with a compact persistent radio source, *arXiv e-prints* arXiv:2110.07418. (2021).
19. E. Fonseca, B. C. Andersen, M. Bhardwaj, P. Chawla, D. C. Good, A. Josephy, V. M. Kaspi, K. W. Masui, R. Mckinven, D. Michilli, Z. Pleunis, K. Shin, S. P. Tendulkar, K. M. Bandura, P. J. Boyle, C. Brar, T. Cassanelli, D. Cubranic, M. Dobbs, F. Q. Dong, B. M. Gaensler, G. Hinshaw, T. L. Landecker, C. Leung, D. Z. Li, H.-H. Lin, J. Mena-Parra, M. Merryfield, A. Naidu, C. Ng, C. Patel, U. Pen, M. Rafiei-Ravandi, M. Rahman, S. M. Ransom, P. Scholz, K. M. Smith, I. H. Stairs, K. Vanderlinde, P. Yadav, and A. V. Zwaniga, Nine New Repeating Fast Radio Burst Sources from CHIME/FRB, *The Astrophysical Journal* **891**, L6. (2020). 10.3847/2041-8213/ab7208
 20. Chime/Frb Collabortion, Recent high activity from a repeating Fast Radio Burst discovered by CHIME/FRB, *The Astronomer's Telegram* **14497**. (2021).
 21. S. Johnston and M. Kerr, Polarimetry of 600 pulsars from observations at 1.4 GHz with the Parkes radio telescope, *Monthly Notices of the Royal Astronomical Society* **474**, 4629-4636. (2018). 10.1093/mnras/stx3095
 22. S. A. Petrova, On the origin of orthogonal polarization modes in pulsar radio emission, *Astronomy and Astrophysics* **378**, 883-897. (2001). 10.1051/0004-6361:20011297
 23. S. P. O'Sullivan, S. Brown, T. Robishaw, D. H. F. M. Schnitzeler, N. M. McClure-Griffiths, I. J. Feain, A. R. Taylor, B. M. Gaensler, T. L. Landecker, L. Harvey-Smith, and E. Carretti, Complex Faraday depth structure of active galactic nuclei as revealed by broad-band radio polarimetry, *Monthly Notices of the Royal Astronomical Society* **421**, 3300-3315. (2012). 10.1111/j.1365-2966.2012.20554.x

24. X. P. You, R. N. Manchester, W. A. Coles, G. B. Hobbs, and R. Shannon, Polarimetry of the Eclipsing Pulsar PSR J1748-2446A, *The Astrophysical Journal* **867**, 22. (2018). 10.3847/1538-4357/aadee0
25. E. J. Polzin, R. P. Breton, B. W. Stappers, B. Bhattacharyya, G. H. Janssen, S. Osłowski, M. S. E. Roberts, and C. Sobey, Long-term variability of a black widow's eclipses - A decade of PSR J2051-0827, *Monthly Notices of the Royal Astronomical Society* **490**, 889-908. (2019). 10.1093/mnras/stz2579
26. M. Xue, S. M. Ord, S. E. Tremblay, N. D. R. Bhat, C. Sobey, B. W. Meyers, S. J. McSweeney, and N. A. Swainston, MWA tied-array processing II: Polarimetric verification and analysis of two bright southern pulsars, *Publications of the Astronomical Society of Australia* **36**, e025. (2019). 10.1017/pasa.2019.19
27. Z. Pleunis, D. Michilli, C. G. Bassa, J. W. T. Hessels, A. Naidu, B. C. Andersen, P. Chawla, E. Fonseca, A. Gopinath, V. M. Kaspi, V. I. Kondratiev, D. Z. Li, M. Bhardwaj, P. J. Boyle, C. Brar, T. Cassanelli, Y. Gupta, A. Josephy, R. Karuppusamy, A. Keimpema, F. Kirsten, C. Leung, B. Marcote, K. W. Masui, R. Mckinven, B. W. Meyers, C. Ng, K. Nimmo, Z. Paragi, M. Rahman, P. Scholz, K. Shin, K. M. Smith, I. H. Stairs, and S. P. Tendulkar, LOFAR Detection of 110-188 MHz Emission and Frequency-dependent Activity from FRB 20180916A, *The Astrophysical Journal* **911**, L3. (2021). 10.3847/2041-8213/abec72
28. G. H. Hilmarsson, D. Michilli, L. G. Spitler, R. S. Wharton, P. Demorest, G. Desvignes, K. Gourdji, S. Hackstein, J. W. T. Hessels, K. Nimmo, A. D. Seymour, M. Kramer, and R. Mckinven, Rotation Measure Evolution of the Repeating Fast Radio Burst Source FRB 121102, *The Astrophysical Journal* **908**, L10. (2021). 10.3847/2041-8213/abdec0

29. G. H. Hilmarsson, L. G. Spitler, R. A. Main, and D. Z. Li, Polarization properties of FRB 20201124A from detections with the Effelsberg 100-m radio telescope, *Monthly Notices of the Royal Astronomical Society* **508**, 5354-5361. (2021). 10.1093/mnras/stab2936
30. Detailed modeling and discussions can be found in supplementary text.
31. Yang, Y.-P., Q.-C. Li, and B. Zhang, Are Persistent Emission Luminosity and Rotation Measure of Fast Radio Bursts Related?, *The Astrophysical Journal* **895**, 7. (2020). 10.3847/1538-4357/ab88ab
32. R. M. Prestage, M. Bloss, J. Brandt, H. Chen, R. Creager, P. Demorest, J. Ford, G. Jones, A. Kepley, A. Kobelski, P. Marganian, M. Mello, D. McMahon, R. McCullough, J. Ray, D. A. Roshi, D. Werthimer, and M. Whitehead, The versatile GBT astronomical spectrometer (VEGAS): Current status and future plans, *2015 URSI-USNC Radio Science Meeting 4*. (2015). 10.1109/USNC-URSI.2015.7303578
33. A. W. Hotan, W. van Straten, and R. N. Manchester, PSRCHIVE and PSRFITS: An Open Approach to Radio Pulsar Data Storage and Analysis, *Publications of the Astronomical Society of Australia* **21**, 302-309. (2004). 10.1071/AS04022
34. S. M. Ransom, New search techniques for binary pulsars, *Ph.D. Thesis* . (2001).
35. P. Jiang, Y. Yue, H. Gan, R. Yao, H. Li, G. Pan, J. Sun, D. Yu, H. Liu, N. Tang, L. Qian, J. Lu, J. Yan, B. Peng, S. Zhang, Q. Wang, Q. Li, and D. Li, Commissioning progress of the FAST, *Science China Physics, Mechanics, and Astronomy* **62**, 959502. (2019). 10.1007/s11433-018-9376-1
36. C.-H. Niu, D. Li, R. Luo, W.-Y. Wang, J. Yao, B. Zhang, W.-W. Zhu, P. Wang, H. Ye, Y.-K. Zhang, J.-. rui . Niu, N.-. yu . Tang, R. Duan, M. Krco, S. Dai, Y. Feng, C. Miao, Z.

- Pan, L. Qian, M. Xue, M. Yuan, Y. Yue, L. Zhang, and X. Zhang, CRAFTS for Fast Radio Bursts: Extending the Dispersion-Fluence Relation with New FRBs Detected by FAST, *The Astrophysical Journal* **909**, L8. (2021). 10.3847/2041-8213/abe7f0
37. B. R. Barsdell, M. Bailes, D. G. Barnes, and C. J. Fluke, Accelerating incoherent dedispersion, *Monthly Notices of the Royal Astronomical Society* **422**, 379-392. (2012). 10.1111/j.1365-2966.2012.20622.x
38. A. Dunning, M. Bowen, S. Castillo, Y. S. Chung, P. Doherty, D. George, D. B. Hayman, K. Jeganathan, H. Kanoniuk, S. Mackay, L. Reilly, P. Roush, S. K. W. Smart, R. D. Shaw, S. L. Smith, T. Tzioumis, V.-C. J. Venables, Design and Laboratory Testing of the Five Hundred Meter Aperture Spherical Telescope (FAST) 19 Beam L-Band Receiver *In 2017 XXXIInd General Assembly and Scientific Symposium of the International Union of Radio Science (URSI GASS)*, 1–4. (2017). 10.23919/URSIGASS.2017.8105012
39. S. Dai, G. Hobbs, R. N. Manchester, M. Kerr, R. M. Shannon, W. van Straten, A. Mata, M. Bailes, N. D. R. Bhat, S. Burke-Spolaor, W. A. Coles, S. Johnston, M. J. Keith, Y. Levin, S. Osłowski, D. Reardon, V. Ravi, J. M. Sarkissian, C. Tiburzi, L. Toomey, H. G. Wang, J.-B. Wang, L. Wen, R. X. Xu, W. M. Yan, and X.-J. Zhu, A study of multifrequency polarization pulse profiles of millisecond pulsars, *Monthly Notices of the Royal Astronomical Society* **449**, 3223-3262. (2015). 10.1093/mnras/stv508
40. B. J. Burn, On the depolarization of discrete radio sources by Faraday dispersion, *Monthly Notices of the Royal Astronomical Society* **133**, 67. (1966). 10.1093/mnras/133.1.67
41. M. A. Brentjens and A. G. de Bruyn, Faraday rotation measure synthesis, *Astronomy and Astrophysics* **441**, 1217-1228. (2005). 10.1051/0004-6361:20052990

42. Everett, J. E. and J. M. Weisberg, Emission Beam Geometry of Selected Pulsars Derived from Average Pulse Polarization Data, *The Astrophysical Journal* **553**, 341-357. (2001). 10.1086/320652
43. C. Sotomayor-Beltran, C. Sobey, J. W. T. Hessels, G. de Bruyn, A. Noutsos, A. Alexov, J. Anderson, A. Asgekar, I. M. Avruch, R. Beck, M. E. Bell, M. R. Bell, M. J. Bentum, G. Bernardi, P. Best, L. Birzan, A. Bonafede, F. Breitling, J. Broderick, W. N. Brouw, M. Brüggen, B. Ciardi, F. de Gasperin, R.-J. Dettmar, A. van Duin, S. Duscha, J. Eislöffel, H. Falcke, R. A. Fallows, R. Fender, C. Ferrari, W. Frieswijk, M. A. Garrett, J. Grießmeier, T. Grit, A. W. Gunst, T. E. Hassall, G. Heald, M. Hoeft, A. Horneffer, M. Iacobelli, E. Juette, A. Karastergiou, E. Keane, J. Kohler, M. Kramer, V. I. Kondratiev, L. V. E. Koopmans, M. Kuniyoshi, G. Kuper, J. van Leeuwen, P. Maat, G. Macario, S. Markoff, J. P. McKean, D. D. Mulcahy, H. Munk, E. Orru, H. Paas, M. Pandey-Pommier, M. Pilia, R. Pizzo, A. G. Polatidis, W. Reich, H. Röttgering, M. Serylak, J. Sluman, B. W. Stappers, M. Tagger, Y. Tang, C. Tasse, S. ter Veen, R. Vermeulen, R. J. van Weeren, R. A. M. J. Wijers, S. J. Wijnholds, M. W. Wise, O. Wucknitz, S. Yatawatta, and P. Zarka, Calibrating high-precision Faraday rotation measurements for LOFAR and the next generation of low-frequency radio telescopes, *Astronomy and Astrophysics* **552**, A58. (2013). 10.1051/0004-6361/201220728
44. F. Vazza, M. Brüggen, P. M. Hinz, D. Wittor, N. Locatelli, and C. Gheller, Probing the origin of extragalactic magnetic fields with Fast Radio Bursts, *Monthly Notices of the Royal Astronomical Society* **480**, 3907-3915. (2018). 10.1093/mnras/sty1968
45. N. Oppermann, H. Junklewitz, M. Greiner, T. A. Enßlin, T. Akahori, E. Carretti, B. M. Gaensler, A. Goobar, L. Harvey-Smith, M. Johnston-Hollitt, L. Pratley, D. H. F. M. Schnitzeler, J. M. Stil, and V. Vacca, Estimating extragalactic Faraday rotation, *Astronomy and Astrophysics* **575**, A118. (2015). 10.1051/0004-6361/201423995

46. P. Beniamini, P. Kumar, and R. Narayan, Faraday depolarization and induced circular polarization by multipath propagation with application to FRBs, *Monthly Notices of the Royal Astronomical Society* **510**, 4654-4668. (2022). 10.1093/mnras/stab3730
47. S. P. Reynolds, B. M. Gaensler, and F. Bocchino, Magnetic Fields in Supernova Remnants and Pulsar-Wind Nebulae, *Space Science Reviews* **166**, 231-261. (2012). 10.1007/s11214-011-9775-y
48. Yang, Y.-P. & Zhang, B., Dispersion Measure Variation of Repeating Fast Radio Burst Sources, *The Astrophysical Journal*, **847**, 22. (2017). 10.3847/1538-4357/aa8721
49. P. Kumar, R. M. Shannon, S. Osłowski, H. Qiu, S. Bhandari, W. Farah, C. Flynn, M. Kerr, D. R. Lorimer, J.-P. Macquart, C. Ng, C. J. Phillips, D. C. Price, and R. Spiewak, Faint Repetitions from a Bright Fast Radio Burst Source, *The Astrophysical Journal* **887**, L30. (2019). 10.3847/2041-8213/ab5b08
50. CHIME/FRB Collaboration, B. C. Andersen, K. Bandura, M. Bhardwaj, P. Boubel, M. M. Boyce, P. J. Boyle, C. Brar, T. Cassanelli, P. Chawla, D. Cubranic, M. Deng, M. Dobbs, M. Fandino, E. Fonseca, B. M. Gaensler, A. J. Gilbert, U. Giri, D. C. Good, M. Halpern, A. S. Hill, G. Hinshaw, C. Höfer, A. Josephy, V. M. Kaspi, R. Kothes, T. L. Landecker, D. A. Lang, D. Z. Li, H.-H. Lin, K. W. Masui, J. Mena-Parra, M. Merryfield, R. Mckinven, D. Michilli, N. Milutinovic, A. Naidu, L. B. Newburgh, C. Ng, C. Patel, U. Pen, T. Pinsonneault-Marotte, Z. Pleunis, M. Rafiei-Ravandi, M. Rahman, S. M. Ransom, A. Renard, P. Scholz, S. R. Siegel, S. Singh, K. M. Smith, I. H. Stairs, S. P. Tendulkar, I. Tretyakov, K. Vanderlinde, P. Yadav, and A. V. Zwaniga, CHIME/FRB Discovery of Eight New Repeating Fast Radio Burst Sources, *The Astrophysical Journal* **885**, L24. (2019). 10.3847/2041-8213/ab4a80

51. C. K. Day, A. T. Deller, R. M. Shannon, H. Qiu, K. W. Bannister, S. Bhandari, R. Ekers, C. Flynn, C. W. James, J.-P. Macquart, E. K. Mahony, C. J. Phillips, and J. Xavier Prochaska, High time resolution and polarization properties of ASKAP-localized fast radio bursts, *Monthly Notices of the Royal Astronomical Society* **497**, 3335-3350. (2020). 10.1093/mnras/staa2138
52. K. Masui, H.-H. Lin, J. Sievers, C. J. Anderson, T.-C. Chang, X. Chen, A. Ganguly, M. Jarvis, C.-Y. Kuo, Y.-C. Li, Y.-W. Liao, M. McLaughlin, U.-L. Pen, J. B. Peterson, A. Roman, P. T. Timbie, T. Voytek, and J. K. Yadav, Dense magnetized plasma associated with a fast radio burst, *Nature* **528**, 523-525. (2015). 10.1038/nature15769
53. E. Petroff, M. Bailes, E. D. Barr, B. R. Barsdell, N. D. R. Bhat, F. Bian, S. Burke-Spolaor, M. Caleb, D. Champion, P. Chandra, G. Da Costa, C. Delvaux, C. Flynn, N. Gehrels, J. Greiner, A. Jameson, S. Johnston, M. M. Kasliwal, E. F. Keane, S. Keller, J. Kocz, M. Kramer, G. Leloudas, D. Malesani, J. S. Mulchaey, C. Ng, E. O. Ofek, D. A. Perley, A. Possenti, B. P. Schmidt, Y. Shen, B. Stappers, P. Tisserand, W. van Straten, and C. Wolf, A real-time fast radio burst: polarization detection and multiwavelength follow-up, *Monthly Notices of the Royal Astronomical Society* **447**, 246-255. (2015). 10.1093/mnras/stu2419
54. E. Petroff, S. Burke-Spolaor, E. F. Keane, M. A. McLaughlin, R. Miller, I. Andreoni, M. Bailes, E. D. Barr, S. R. Bernard, S. Bhandari, N. D. R. Bhat, M. Burgay, M. Caleb, D. Champion, P. Chandra, J. Cooke, V. S. Dhillon, J. S. Farnes, L. K. Hardy, P. Jaroenjittichai, S. Johnston, M. Kasliwal, M. Kramer, S. P. Littlefair, J. P. Macquart, M. Mickaliger, A. Possenti, T. Pritchard, V. Ravi, A. Rest, A. Rowlinson, U. Sawangwit, B. Stappers, M. Sullivan, C. Tiburzi, W. van Straten, ANTARES Collaboration, A. Albert, M. André, M. Anghinolfi, G. Anton, M. Ardid, J.-J. Aubert, T. Avgitas, B. Baret, J. Barrios-Martí, S. Basa, V. Bertin, S. Biagi, R. Bormuth, S. Bourret, M. C. Bouwhuis, R. Bruijn, J. Brunner,

J. Busto, A. Capone, L. Caramete, J. Carr, S. Celli, T. Chiarusi, M. Circella, J. A. B. Coelho, A. Coleiro, R. Coniglione, H. Costantini, P. Coyle, A. Creusot, A. Deschamps, G. de Bonis, C. Distefano, I. di Palma, C. Donzaud, D. Dornic, D. Drouhin, T. Eberl, I. El Bojaddaini, D. Elsässer, A. Enzenhöfer, I. Felis, L. A. Fusco, S. Galatà, P. Gay, S. Geißelsöder, K. Geyer, V. Giordano, A. Gleixner, H. Glotin, T. Grégoire, R. Gracia-Ruiz, K. Graf, S. Hallmann, H. van Haren, A. J. Heijboer, Y. Hello, J. J. Hernández-Rey, J. Höbl, J. Hofestädt, C. Hugon, G. Illuminati, C. W. James, M. de Jong, M. Jongen, M. Kadler, O. Kalekin, U. Katz, D. Kießling, A. Kouchner, M. Kreter, I. Kreykenbohm, V. Kulikovskiy, C. Lachaud, R. Lahmann, D. Lefèvre, E. Leonora, M. Lotze, S. Loucatos, M. Marcelin, A. Margiotta, A. Marinelli, J. A. Martínez-Mora, A. Mathieu, R. Mele, K. Melis, T. Michael, P. Migliozi, A. Moussa, C. Mueller, E. Nezri, G. E. Pāvāļš, C. Pellegrino, C. Perrina, P. Piattelli, V. Popa, T. Pradier, L. Quinn, C. Racca, G. Riccobene, K. Roensch, A. Sánchez-Losa, M. Saldaña, I. Salvadori, D. F. E. Samtleben, M. Sanguineti, P. Sapienza, J. Schnabel, T. Seitz, C. Sieger, M. Spurio, T. Stolarczyk, M. Taiuti, Y. Tayalati, A. Trovato, M. Tselengidou, D. Turpin, C. Tönnis, B. Vallage, C. Vallée, V. van Elewyck, D. Vivolo, A. Vizzoca, S. Wagner, J. Wilms, J. D. Zornoza, J. Zúñiga, H. E. S. S. Collaboration, H. Abdalla, A. Abramowski, F. Aharonian, F. Ait Benkhali, A. G. Akhperjanian, T. Andersson, E. O. Angüner, M. Arrieta, P. Aubert, M. Backes, A. Balzer, M. Barnard, Y. Becherini, J. B. Tjus, D. Berge, S. Bernhard, K. Bernlöhr, R. Blackwell, M. Böttcher, C. Boisson, J. Bolmont, P. Bordas, J. Bregeon, F. Brun, P. Brun, M. Bryan, T. Bulik, M. Capasso, S. Casanova, M. Cerruti, N. Chakraborty, R. Chalme-Calvet, R. C. G. Chaves, A. Chen, J. Chevalier, M. Chrétien, S. Colafrancesco, G. Cologna, B. Condon, J. Conrad, Y. Cui, I. D. Davids, J. Decock, B. Degrange, C. Deil, J. Devin, P. Dewilt, L. Dirson, A. Djannati-Ataï, W. Domainko, A. Donath, L. O. Drury, G. Dubus, K. Dutson, J. Dyks, T. Edwards, K. Egberts, P. Eger, J.-P. Ernenwein, S. Eschbach, C. Farnier, S. Fegan, M. V. Fernandes, A. Fiasson, G. Fontaine, A. Förster, S. Funk, M.

Füßling, S. Gabici, M. Gajdus, Y. A. Gallant, T. Garrigoux, G. Giavitto, B. Giebels, J. F. Glicenstein, D. Gottschall, A. Goyal, M.-H. Grondin, D. Hadasch, J. Hahn, M. Haupt, J. Hawkes, G. Heinzelmann, G. Henri, G. Hermann, O. Hervet, J. A. Hinton, W. Hofmann, C. Hoischen, M. Holler, D. Horns, A. Ivascenko, A. Jacholkowska, M. Jamrozy, M. Jankowski, D. Jankowsky, F. Jankowsky, M. Jingo, T. Jogler, L. Jouvin, I. Jung-Richardt, M. A. Kastendieck, K. Katarzyński, D. Kerszberg, B. Khélifi, M. Kieffer, J. King, S. Klepser, D. Klochkov, W. Kluźniak, D. Kolitzus, N. Komin, K. Kosack, S. Krakau, M. Kraus, F. Krayzel, P. P. Krüger, H. Laffon, G. Lamanna, J. Lau, J.-P. Lees, J. Lefaucheur, V. Lefranc, A. Lemièrre, M. Lemoine-Goumard, J.-P. Lenain, E. Leser, T. Lohse, M. Lorentz, R. Liu, R. López-Coto, I. Lypova, V. Marandon, A. Marcowith, C. Mariaud, R. Marx, G. Maurin, N. Maxted, M. Mayer, P. J. Meintjes, M. Meyer, A. M. W. Mitchell, R. Moderski, M. Mohamed, L. Mohrmann, K. Morâ, E. Moulin, T. Murach, M. de Naurois, F. Niederwanger, J. Niemiec, L. Oakes, P. O'Brien, H. Odaka, S. Öttl, S. Ohm, M. Ostrowski, I. Oya, M. Padovani, M. Panter, R. D. Parsons, N. W. Pekeur, G. Pelletier, C. Perennes, P.-O. Petrucci, B. Peyaud, Q. Piel, S. Pita, H. Poon, D. Prokhorov, H. Prokoph, G. Pühlhofer, M. Punch, A. Quirrenbach, S. Raab, A. Reimer, O. Reimer, M. Renaud, R. D. L. Reyes, F. Rieger, C. Romoli, S. Rosier-Lees, G. Rowell, B. Rudak, C. B. Rulten, V. Sahakian, D. Salek, D. A. Sanchez, A. Santangelo, M. Sasaki, R. Schlickeiser, A. Schulz, F. Schüssler, U. Schwanke, S. Schwemmer, M. Settimo, A. S. Seyffert, N. Shafi, I. Shilon, R. Simoni, H. Sol, F. Spanier, G. Spengler, F. Spies, Ł. Stawarz, R. Steenkamp, C. Stegmann, F. Stinzing, K. Stycz, I. Sushch, J.-P. Tavernet, T. Tavernier, A. M. Taylor, R. Terrier, L. Tibaldo, D. Tiziani, M. Tluczykont, C. Trichard, R. Tuffs, Y. Uchiyama, D. J. V. D. Walt, C. van Eldik, C. van Rensburg, B. van Soelen, G. Vasileiadis, J. Veh, C. Venter, A. Viana, P. Vincent, J. Vink, F. Voisin, H. J. Völk, T. Vuillaume, Z. Wadiasingh, S. J. Wagner, P. Wagner, R. M. Wagner, R. White, A. Wierzcholska, P. Willmann, A. Wörnlein, D. Wouters, R. Yang, V.

- Zabalza, D. Zaborov, M. Zacharias, R. Zanin, A. A. Zdziarski, A. Zech, F. Zefi, A. Ziegler, and N. Żywucka, A polarized fast radio burst at low Galactic latitude, *Monthly Notices of the Royal Astronomical Society* **469**, 4465-4482. (2017). 10.1093/mnras/stx1098
55. E. F. Keane, S. Johnston, S. Bhandari, E. Barr, N. D. R. Bhat, M. Burgay, M. Caleb, C. Flynn, A. Jameson, M. Kramer, E. Petroff, A. Possenti, W. van Straten, M. Bailes, S. Burke-Spolaor, R. P. Eatough, B. W. Stappers, T. Totani, M. Honma, H. Furusawa, T. Hattori, T. Morokuma, Y. Niino, H. Sugai, T. Terai, N. Tominaga, S. Yamasaki, N. Yasuda, R. Allen, J. Cooke, J. Jencson, M. M. Kasliwal, D. L. Kaplan, S. J. Tingay, A. Williams, R. Wayth, P. Chandra, D. Perrodin, M. Berezina, M. Mickaliger, and C. Bassa, The host galaxy of a fast radio burst, *Nature* **530**, 453-456. (2016). 10.1038/nature17140
56. V. Ravi, R. M. Shannon, M. Bailes, K. Bannister, S. Bhandari, N. D. R. Bhat, S. Burke-Spolaor, M. Caleb, C. Flynn, A. Jameson, S. Johnston, E. F. Keane, M. Kerr, C. Tiburzi, A. V. Tuntsov, and H. K. Vedantham, The magnetic field and turbulence of the cosmic web measured using a brilliant fast radio burst, *Science* **354**, 1249-1252. (2016). 10.1126/science.aaf6807
57. M. Caleb, E. F. Keane, W. van Straten, M. Kramer, J. P. Macquart, M. Bailes, E. D. Barr, N. D. R. Bhat, S. Bhandari, M. Burgay, W. Farah, A. Jameson, F. Jankowski, S. Johnston, E. Petroff, A. Possenti, B. W. Stappers, C. Tiburzi, and V. Venkatraman Krishnan, The SURvey for Pulsars and Extragalactic Radio Bursts - III. Polarization properties of FRBs 160102 and 151230, *Monthly Notices of the Royal Astronomical Society* **478**, 2046-2055. (2018). 10.1093/mnras/sty1137
58. H. Cho, J.-P. Macquart, R. M. Shannon, A. T. Deller, I. S. Morrison, R. D. Ekers, K. W. Bannister, W. Farah, H. Qiu, M. W. Sammons, M. Bailes, S. Bhandari, C. K. Day, C. W. James, C. J. Phillips, J. X. Prochaska, and J. Tuthill, Spectropolarimetric Analysis of FRB

181112 at Microsecond Resolution: Implications for Fast Radio Burst Emission Mechanism, *The Astrophysical Journal* **891**, L38. (2020). 10.3847/2041-8213/ab7824

59. <https://www.wis-tns.org>

60. M. Amiri, B. C. Andersen, K. Bandura, S. Berger, M. Bhardwaj, M. M. Boyce, P. J. Boyle, C. Brar, D. Breitman, T. Cassanelli, P. Chawla, T. Chen, J.-F. Cliche, A. Cook, D. Cubranic, A. P. Curtin, M. Deng, M. Dobbs, F. (Adam) Dong, G. Eadie, M. Fandino, E. Fonseca, B. M. Gaensler, U. Giri, D. C. Good, M. Halpern, A. S. Hill, G. Hinshaw, A. Josephy, J. F. Kaczmarek, Z. Kader, J. W. Kania, V. M. Kaspi, T. L. Landecker, D. Lang, C. Leung, D. Li, H.-H. Lin, K. W. Masui, R. McKinven, J. Mena-Parra, M. Merryfield, B. W. Meyers, D. Michilli, N. Milutinovic, A. Mirhosseini, M. Münchmeyer, A. Naidu, L. Newburgh, C. Ng, C. Patel, U.-L. Pen, E. Petroff, T. Pinsonneault-Marotte, Z. Pleunis, M. Rafei-Ravandi, M. Rahman, S. M. Ransom, A. Renard, P. Sanghavi, P. Scholz, J. R. Shaw, K. Shin, S. R. Siegel, A. E. Sikora, S. Singh, K. M. Smith, I. Stairs, C. M. Tan, S. P. Tendulkar, K. Vanderlinde, H. Wang, D. Wulf, A. V. Zwaniga, and CHIME/FRB Collaboration, The First CHIME/FRB Fast Radio Burst Catalog, *The Astrophysical Journal Supplement Series* **257**, 59. (2021). 10.3847/1538-4365/ac33ab

61. G. B. Hobbs, R. T. Edwards, and R. N. Manchester, TEMPO2, a new pulsar-timing package - I. An overview, *Monthly Notices of the Royal Astronomical Society* **369**, 655-672. (2006). 10.1111/j.1365-2966.2006.10302.x

Acknowledgments

We thank Brenne Gregory for help with the observations and Emmanuel Fonseca, G. H. Hilmarsson, Daniele Michilli, Jason Hessels, Adam Deller, Cherie Day, Steve White and Bob Simon for valuable discussions. This work made use of data from FAST, a Chinese national mega-science

facility, operated by National Astronomical Observatories, Chinese Academy of Sciences. The Green Bank Observatory is a facility of the National Science Foundation operated under cooperative agreement by Associated Universities, Inc.

Funding

D.L. and Y.F. are supported by NSFC grant No. 11988101, 11725313, 11690024, by the National Key R&D Program of China No. 2017YFA0402600, and by Key Research Project of Zhejiang Lab No. 2021PE0AC03. Y.P.Y is supported by NSFC grant No. 12003028. W.W.Z. is supported by National SKA Program of China No.2020SKA0120200 and the NSFC 12041303, 11873067. W.B.L. is supported by Lyman Spitzer, Jr. Fellowship at Princeton University. P.W. is supported by NSFC grant No. U2031117, the Youth Innovation Promotion Association CAS (id. 2021055), CAS Project for Young Scientists in Basic Research (grant YSBR-006) and the Cultivation Project for FAST Scientific Payoff and Research Achievement of CAMS-CAS. S. D. is the recipient of an Australian Research Council Discovery Early Career Award (DE210101738) funded by the Australian Government. J.M.Y. is supported by NSFC grant No. 11903049, and the Cultivation Project for FAST Scientific Payoff and Research Achievement of CAMS-CAS. L.Q. is supported by National SKA Program of China No. 2020SKA0120100 and the Youth Innovation Promotion Association of CAS (id. 2018075). S.B.Z. is supported by NSFC grant No. 12041306, and by China Postdoctoral Science Foundation (Grant No. 2020M681758). L.Z. is supported by NSFC grant No. 12103069.

Author Contributions

Y.F. and D.L. developed the concept of the manuscript. Y.F. and D.L. led the discussion on the interpretation of the results and writing of the manuscript. Y.P.Y., B.Z. and W.B.L. derived the theoretical formula. Y.F., D.L., W.W.Z., B.Z., W.B.L., R.S.L. and C.H.N. arranged the

observations. Y.F. and Y.K.Z. conducted the main data analysis and visualization. All authors contributed to the analysis or interpretation of the data and to the final version of the manuscript.

Competing interests

The authors declare no competing interests.

Data and materials availability

Observational data of FAST (Project ID: ZD2020_5) are available from the FAST archive (<http://fast.bao.ac.cn>) 1 year after data collection, following FAST data policy. Observational data of GBT (Project ID: 21A-404 and 21A-416) are available from the GBT archive (<https://greenbankobservatory.org>) 1 year after data collection, following GBT data policy. The archival data sources are listed in Table S1. The numerical results of the analysis are listed in Tables S2 and S3. The bursts data for Tables S2 and S3 are openly available in Science Data Bank at <https://doi.org/10.11922/sciencedb.o00069.00006>. Computational programs for the polarization analysis reported here are available at <https://github.com/SukiYume/RMS>. Other standard data reduction packages are available at their respective websites: PRESTO (<https://github.com/scottransom/presto>), HEIMDALL (<http://sourceforge.net/projects/heimdall-astro/>), PSRCHIVE (<http://psrchive.sourceforge.net>).

Supplementary materials

Materials and Methods

Supplementary Text

Figs. S1 to S5

Tables. S1 to S3

References (32-61)

Supplementary Materials for

Frequency Dependent Polarization of Repeating Fast Radio Bursts -
Implications for Their Origin

Yi Feng, Di Li, Yuan-Pei Yang, Yongkun Zhang, Weiwei Zhu, Bing Zhang,
Wenbin Lu, Pei Wang, Shi Dai, Ryan S. Lynch, Jumei Yao, Jinchun Jiang,
Jiarui Niu, Dejiang Zhou, Heng Xu, Chenchen Miao, Chenhui Niu,
Lingqi Meng, Lei Qian, Chao-Wei Tsai, Bojun Wang, Mengyao Xue,
Youling Yue, Mao Yuan, Songbo Zhang, Lei Zhang

Correspondence to: dili@nao.cas.cn

This PDF file includes:

Materials and Methods

Supplementary Text

Figs. S1 to S5

Tables S1 to S3

Materials and Methods

S1 Observations and burst detection

S1.1 FRB 20190520B

FRB 20190520B was observed from 3.95–7.8 GHz with the GBT’s C-Band receiver and the Versatile Green Bank Astronomical Spectrometer (VEGAS) digital backend (32). VEGAS consists of eight spectrometer banks, each of which can sample 1.5 GHz of bandwidth, though filters reduce the usable bandwidth to 1.25 GHz per bank. In the case of FRB 20190520B, we used four VEGAS banks centered on 4312.5, 5437.5, 6562.5, and 7687.5 GHz. Each of these sub-bands overlapped the next by 187.5 MHz, ensuring complete sampling over the frequencies of interest. The data were then combined in post-processing to cover the full available receiver band.

Data were recorded in the PSRFITS standard format (33). Full-Stokes spectra were recorded every 43.907 μs with 0.366 MHz-wide channels (i.e., 4096 channels per spectrometer bank).

We searched for bursts with widths up to 10 ms in dedispersed time series using a matched filtering algorithm as implemented by the PRESTO program (34) SINGLE_PULSE_SEARCH.PY. We retained the native sampling rate of the full-resolution data but reduced the frequency resolution by a factor of four to increase computational efficiency. Using wider channel bandwidths leads to slightly more intra-channel dispersive smearing, but the effect is not large. For example, at the lowest frequency in our observing band (3.95 GHz) the dispersive smearing at our native frequency resolution is 0.06 ms, and in the reduced-resolution data it is 0.2 ms, which is still much less than the typical FRB pulse width. The data were then dedispersed using the PRESTO program PREPSUBBAND at dispersion measures (DMs) ranging from 1110–1309 pc cm^{-3} with a step size of 1 pc cm^{-3} . Searching for bursts over a range of DMs allowed us to differentiate between astrophysical sources and radio frequency interference by looking for a characteristic

peak in signal to noise ratio (S/N) near the true DM of the FRB and a monotonically decreasing S/N as the error in DM increases. We examined all candidate bursts with $S/N > 6$ to confirm or reject their astrophysical nature.

Data were calibrated using the PSRCHIVE package (33). On and off-source observations of the standard calibrator 3C 394 were used to measure the intensity of the C-Band receiver’s built-in noise diode. The noise diode was observed again at the position of FRB 20190520B prior to the main observations, and these data were used to calibrate each burst from the FRB.

S1.2 FRB 20190303A

Observations of FRB 20190303A were carried out using the FAST telescope mounted with the 19-beam receiver (35), which operates with a frequency range from 1050-1450 MHz and provides two data streams (one for each linear polarization). The data streams are processed with the Reconfigurable Open Architecture Computing Hardware–version 2 (ROACH2) signal processor (35). The output data files are recorded as 8 bit-sampled search mode PSRFITS files with 4096 frequency channels.

Observations were carried out in six sessions. We carried out the first and second session on 4 Jan 2021 and 5 Jan 2021 to do a 2-hour gridding observation using all beams of the 19-beam receiver. $196.608 \mu\text{s}$ time resolution was used. The central beam of the receiver was initially placed on the previously reported position (RA = 13h53min, Dec = $+48^\circ 15'$) (J2000) (19). Figure S1 shows the first gridding observation of FRB 20190303A on 4 Jan 2021 and 5 Jan 2021. One burst was detected in Beam M13 of the N3 pointing with position of (RA = $13^{\text{h}}51^{\text{m}}58^{\text{s}}$, Dec = $48^\circ 07' 20''$) (J2000).

We then carried out the third and fourth session on 19 Jan 2021 and 20 Jan 2021 to do a second 2-hour gridding observation. $98.304 \mu\text{s}$ time resolution was used. The central beam of the receiver was initially placed on the position of the first detection. One burst was detected in

Beam M01 of the N1 pointing, i.e. the position of the first detection.

Because we did not detect any burst signal in other beams, we take (RA = $13^h 51^m 58^s$, Dec = $+48^\circ 07' 20''$) (J2000) as the probable FRB position and carried out another two observations using only the central beam placed on the probable FRB position. 49.152 μ s time resolution was used. The fifth session on 3 Feb 2021 lasted for two hours and no bursts were detected. The sixth session on 14 Feb 2021 lasted for one hour and two bursts were detected.

The tracking data was searched using the FAST_MINER pipeline (36). The data stream from each beam was processed using HEIMDALL (37), which dedisperses the data incoherently with DM ranging between 20 and 2000 pc cm^{-3} . We kept the candidates that show less than 4 adjacent beams and S/N greater than 7 for further identification from waterfall plots. From the waterfalls we identified four bursts reported above.

S1.3 FRB 20190417A

The observations of FRB 20190417A were carried out using the FAST telescope mounted with the 19-beam receiver. Observations were carried out in two sessions. We carried out the first and second session on 30 Jul 2020 and 17 Aug 2020 to do a 1-hour observation using all beams of the 19-beam receiver. 49.152 and 98.304 μ s time resolution were used. The central beam of the receiver was initially placed on the previously reported position (RA = 19h39min, Dec = $+59^\circ 24'$) (J2000) (19). Two bursts were detected in Beam M07 with position of (RA = $19^h 39^m 22^s$, Dec = $+59^\circ 18' 58''$) (J2000). The central beam of the receiver was placed on the position of the first detection. 23 bursts were detected in Beam M01, i.e. the position of the first detection.

The tracking data was searched by dedicated and blind search during the observational campaign. We performed 14 box-car pulse width match-filter grids scheduled in logarithmic space from 0.1 to 30 ms using PRESTO. A zero-DM matched filter was applied to mitigate radio fre-

quency interference (RFI) in the blind search. The data were de-dispersed at DMs ranging from 800 to 1800 pc cm^{-3} with the step size of 1 pc cm^{-3} . All of the possible pulse candidates of $S/N > 6$ were plotted, then be confirmed pulse by pulse with dispersive signature to remove the narrow-band RFI.

S1.4 FRB 20201124A

FRB 20201124A was observed with the 800 MHz feed (720–920 MHz) of the GBT’s prime focus receiver and the VEGAS digital backend. The data were coherently dedispersed at a DM of 413.52 pc cm^{-3} and recorded in the PSRFITS standard format. Full polarization self and cross products were recorded every 81.92 μs with 195.3125 kHz-wide channels (i.e., 1024 frequency channels). Data were calibrated using the same procedure as we used for FRB 20190520B, except we used FIRST J141341.6+15093 (aka J1413+1509) as the calibration source.

We searched for bursts using PRESTO in a similar way as with FRB 20190520B, with the main differences being that we retained the full time and frequency resolution and searched DMs ranging from 200–600 pc cm^{-3} with a step size of 1 pc cm^{-3} . 9 bursts were detected.

FRB 20201124A was also observed with the FAST telescope between 1.0 and 1.4 GHz. The data streams were processed with the ROACH2 signal processor and recorded as 8 bit-sampled search mode PSRFITS files with 4096 frequency channels and 49.152 μs sampling time. Using PRESTO, we searched DMs ranging from 200–600 pc cm^{-3} with a step size of 1 pc cm^{-3} , resulting in 11 bursts.

S2 Polarization and Faraday rotation

The bursts were dedispersed using previously published dispersion measures, listed in Table S2. Polarization calibration was performed with the PSRCHIVE software package (33) using the single-axis model. This calibration strategy uses a noise diode to correct for the differential

gain and phase between the two polarization channels. This calibration scheme does not correct for leakage. At FAST, the leakage term is better than -46 dB within the full width at half maximum region of the central beam as measured during the FAST engineering phase (38), which corresponds to systematic errors less than 0.5%. The polarization properties of bright pulsars are consistent between FAST and the Parkes Pulsar Timing Array within 0.5% (39). The cross-polarization leakage of the GBT C-Band receiver when recording linear polarization is < -32 dB over our observed bandwidth, and over most of the band it is < -37 dB, which corresponds to systematic errors of about 1.4%. To excise RFI, we used the PSRCHIVE software package to median filter each burst in the frequency domain and mitigated RFI of each burst manually.

The RM is defined as

$$\text{RM} \equiv 0.81 \int_d^0 \frac{B_{\parallel}(l)n_e(l)}{(1+z)^2} dl, \quad (\text{S1})$$

where l is the line-of-sight position; B_{\parallel} is the line-of-sight magnetic field strength in micro-gauss; n_e is the electron density; z is the redshift of the source; and d is the distance to the source. We report the observed RM and do not correct it for redshift,. We searched for an RM detection using the methods of Stokes QU-fitting (23) and RM-synthesis (40, 41). The RM values of FRB 20190520B, FRB 20190303A, FRB 20190417A, and FRB 20201124A are listed in Table S3. Examples of the results from RM-synthesis for each FRB with RM detection are shown in Figure S2 and for Stokes QU-fitting in Figure S3. We find consistent values with both methods (Table S3).

For FRB 20121102A, we obtained polarization measurements resulting in non-detection of linear polarization at 1.0-1.5 GHz with FAST. We searched for the RM from -3.0×10^5 to 3.0×10^5 rad m⁻² for all bursts of FRB 20121102A at 1.0-1.5 GHz with FAST and we show the RM search for the three brightest bursts in Figure S4. No peak was found in the Faraday spectrum and we place an upper limit of 6% on the degree of linear polarization for FRB 20121102A at

1.25 GHz.

For FRB 20190520B, we obtained polarization measurements resulting in non-detection of linear polarization at 1.0-1.5 GHz with FAST. We searched for the RM from -3.0×10^5 to 3.0×10^5 rad m⁻² for three brightest bursts of FRB 20190520B at 1.0-1.5 GHz with FAST and the result is shown in Figure S4. No peak was found in the Faraday spectrum and we place an upper limit of 20% on the degree of linear polarization for FRB 20190520B at 1.25 GHz. $f_{\text{depol}} = 0.2$ when RM = 10^5 rad/m², therefore the non-detection of linear polarization of FRB 20121102A and 20190520B at 1.0-1.5 GHz is not caused by intra-channel depolarization.

Finally, we calculated the degrees of linear polarization and circular polarization for bursts with RM detection. We first derotated the linear polarization with the measured RM. The representative RM-corrected polarization profiles of FRB 20190303A, FRB 20190520B, FRB 20190417A, and FRB 20201124A are shown in Figure 1. The measured linear polarization is overestimated in the presence of noise. Therefore we use the frequency-averaged, de-biased total linear polarization (42) :

$$L_{\text{de-bias}} = \begin{cases} \sigma_I \sqrt{\left(\frac{L_i}{\sigma_I}\right)^2 - 1} & \text{if } \frac{L_i}{\sigma_I} > 1.57 \\ 0 & \text{otherwise,} \end{cases} \quad (\text{S2})$$

where σ_I is the Stokes I off-pulse standard deviation and L_i is the measured frequency-averaged linear polarization of time sample i . We defined the degree of linear polarization as $(\sum_i L_{\text{de-bias},i})/(\sum_i I_i)$ and that of circular polarization as $(\sum_i V_i)/(\sum_i I_i)$, where the summation is over the bursts and V_i is the measured frequency-averaged circular polarization of time sample i . Defining $I = \sum_i I_i$, $L = \sum_i L_{\text{de-bias},i}$ and $V = \sum_i V_i$, uncertainties on the linear polarization fraction and circular polarization fraction are calculated as:

$$\sigma_{\rho/I} = \frac{\sqrt{N + N \frac{\rho^2}{I^2}}}{I} \sigma_I, \quad (\text{S3})$$

where N is the number of time samples of the burst, and $\rho = L, V$ for linear and circular

polarization fraction, respectively. The degrees of linear polarization and circular polarization are listed in Table S3.

S3 RM budget and σ_{RM}

The observed total rotation measure RM_{tot} is a combination of multiple contributions:

$$\text{RM}_{\text{tot}} = \text{RM}_{\text{iono}} + \text{RM}_{\text{Gal}} + \text{RM}_{\text{IGM}} + \text{RM}_{\text{host}} + \text{RM}_{\text{source}}, \quad (\text{S4})$$

where RM_{iono} is the RM due to the Earth’s ionosphere, RM_{Gal} is the Galactic foreground, RM_{IGM} is the contribution from the intergalactic medium (IGM), RM_{host} is the RM in a host galaxy and $\text{RM}_{\text{source}}$ is the intrinsic component from magnetised plasma associated with the progenitor source and its immediate environment. The observed RM_{host} and $\text{RM}_{\text{source}}$ are smaller by $(1+z)^2$ compared with their rest-frame values (Eq. S1), and our RM budget assumes that the observed values are the same as the rest-frame values to simplify the analysis. RM_{iono} does not exceed a few rad/m^2 (43). RM_{IGM} is typically smaller than $20 \text{ rad}/\text{m}^2$ (44) and RM_{Gal} is typically smaller than $100 \text{ rad}/\text{m}^2$ (45). RM_{host} can be reasonably assumed to be smaller than RM_{Gal} . Thus we assume $\text{RM}_{\text{tot}} = \text{RM}_{\text{source}}$ for the repeaters in our sample.

For each repeater which has bursts with degree of linear polarization less than 90%, we determine σ_{RM} by fitting the data with the model in Eq. 2 assuming each burst has 100% intrinsic linear polarization. For FRB 20201124A, an unweighted least squares fit was used because the FAST measurements have much smaller uncertainties than the GBT data. For other FRBs, an inverse-variance weighted least squares fit was used. For λ in Eq. 2, we calculated the central frequency of each burst weighted by signal-to-noise ratio and converted the weighted frequency to the equivalent wavelength λ . The resulting σ_{RM} values are listed in Table S2. The inferred σ_{RM} is in the observer’s frame. If the source were at a high redshift z , then the true σ_{RM} is higher by a factor of $(1+z)^2$, which is the same scaling as RM. For instance, if FRB 20190417A, which

has a large DM of 1378 pc cm^{-3} (19), is at $z = 1$, then the true σ_{RM} is a factor of 4 larger, making this source similar to FRB 20121102A.

Supplementary Text

S4 RM scatter and temporal scattering caused by a magnetised plasma screen

In this section, we discuss scintillation, temporal scattering, and σ_{RM} from a magneto-ionic inhomogeneous plasma screen near the repeater source, as shown schematically in Figure S5 (see also Ref. (46) for a more detailed treatment). We consider that the plasma screen has a thickness ΔR and a radius R , respectively, and assume $\Delta R \sim R$. The electron density fluctuation is δn_e in the scale δl . $\delta l/R < \theta_s$ is required for scintillation and temporal scattering, where θ_s is the refraction angle from Eq.(S5). When a radio burst propagates in the plasma screen, the variation in phase velocity is approximately $\delta v_{\text{pha}} \simeq c\delta(\omega_p^2)/2\omega^2 = 2\pi e^2 c\delta n_e/m_e\omega^2$ for $\omega \gg \omega_B$, where m_e is the electron rest mass, $\omega_p = (4\pi e^2 n_e/m_e)^{1/2}$ is the plasma frequency, $\omega_B = eB/m_e c$ is the electron cyclotron frequency, and ω is the wave angular frequency. The wavefront is advanced or retarded by $\sim (\delta v_{\text{pha}}/c)\delta l$ relative to propagation in a homogeneous medium, after the wavefront traverses a single clump of lengthscale δl . After traveling through the plasma screen with thickness ΔR , the wavefront has crossed $\Delta R/\delta l$ clumps, and the advance or retardation of the wavefront is $\delta x \sim (\Delta R/\delta l)^{1/2}(\delta v_{\text{pha}}/c)\delta l$. The wavefront surface will be tilted by an angle of $\theta_s \simeq \delta x/\delta l$ due to multiple refraction by clumps, and the characteristic value of the refraction angle is

$$\begin{aligned} \theta_s &\simeq \left(\frac{\Delta R}{\delta l}\right)^{1/2} \frac{e^2}{2\pi m_e \nu^2} \delta n_e = 7.1 \times 10^{-6} \text{ rad} \left(\frac{\Delta R}{1 \text{ pc}}\right)^{1/2} \\ &\times \left(\frac{\delta l}{10^{12} \text{ cm}}\right)^{-1/2} \left(\frac{\delta n_e}{100 \text{ cm}^{-3}}\right) \left(\frac{\nu}{1 \text{ GHz}}\right)^{-2}, \end{aligned} \quad (\text{S5})$$

where $\nu = \omega/2\pi$ is the wave frequency. From Figure S5, the path-length difference between two rays is $\Delta s = R(1 - \cos \theta_s) \simeq R\theta_s^2/2$ for $\theta_s \ll 1$. Thus, the temporal scattering time can be estimated as

$$\begin{aligned} \tau_{\text{sca}} &\simeq \frac{R\theta_s^2}{2c} = 2.6 \text{ ms} \left(\frac{R}{1 \text{ pc}} \right)^2 \\ &\times \left(\frac{\delta l}{10^{12} \text{ cm}} \right)^{-1} \left(\frac{\delta n_e}{100 \text{ cm}^{-3}} \right)^2 \left(\frac{\nu}{1 \text{ GHz}} \right)^{-4}. \end{aligned} \quad (\text{S6})$$

Here, the assumption of $\Delta R \sim R$ is used. For a certain plasma screen, scintillation and temporal scattering occur together and have a relationship of $\Delta\nu_{\text{sci}} = 1/(2\pi\tau_{\text{sca}})$, where $\Delta\nu_{\text{sci}}$ is the scintillation bandwidth. The corresponding scintillation bandwidth is

$$\begin{aligned} \Delta\nu_{\text{sci}} &\simeq \frac{1}{2\pi\tau_{\text{sca}}} = 62 \text{ Hz} \left(\frac{R}{1 \text{ pc}} \right)^{-2} \\ &\times \left(\frac{\delta l}{10^{12} \text{ cm}} \right) \left(\frac{\delta n_e}{100 \text{ cm}^{-3}} \right)^{-2} \left(\frac{\nu}{1 \text{ GHz}} \right)^4, \end{aligned} \quad (\text{S7})$$

This value is much smaller than the observed scintillation bandwidth of $\Delta\nu_{\text{sci}} \sim 1\text{MHz}$. This is consistent with the observed scintillation being more likely contributed by the interstellar medium within the Milky Way.

Next, we discuss the effect of RM scatter. We assume that the magnetic field also has a typical lengthscale δl . The differences of multi-path RMs is large enough to cause depolarization when a radio wave propagates in the magneto-ionic inhomogeneous environment. The decorrelation lengthscale of the fluctuation of Faraday rotation angle could be much larger than that of the fluctuation of wave phase in the plasma screen, because the evolution of the rotation angle is much slower than that of the wave phase for $\omega \gg \omega_B$. Because the large-scale turbulence dominates the Faraday rotation, the decorrelation lengthscale of Faraday rotation angle is

approximately the transverse lengthscale of the visible part of the plasma screen, i.e.,

$$l_{\text{sca}} = \theta_s R = 2.2 \times 10^{13} \text{ cm} \left(\frac{R}{1 \text{ pc}} \right)^{3/2} \\ \times \left(\frac{\delta l}{10^{12} \text{ cm}} \right)^{-1/2} \left(\frac{\delta n_e}{100 \text{ cm}^{-3}} \right) \left(\frac{\nu}{1 \text{ GHz}} \right)^{-2}. \quad (\text{S8})$$

According to the definition of rotation measure, i.e., $\phi \equiv \lambda^2 \text{RM}$, where ϕ is the rotation angle, λ is the wavelength, and RM is the rotation measure, the total RM scatter contributed by the plasma screen could be calculated by

$$\sigma_{\text{RM}} \simeq \sqrt{\frac{\Delta R}{l_{\text{sca}}}} |\text{RM}_{\text{sca}}| = 1.4 \text{ rad m}^{-2} \left(\frac{R}{1 \text{ pc}} \right)^{1/2} \\ \times \left(\frac{\delta(n_e B_{\parallel})}{10^3 \text{ cm}^{-3} \mu\text{G}} \right) \left(\frac{l_{\text{sca}}}{10^{13} \text{ cm}} \right)^{1/2}, \quad (\text{S9})$$

where the RM contribution in a turbulence region with scale l_{sca} is given by

$$\text{RM}_{\text{sca}} = \frac{e^3}{2\pi m_e^2 c^4} \delta(B_{\parallel} n_e) l_{\text{sca}}. \quad (\text{S10})$$

The requirements of $\delta(n_e B_{\parallel}) \sim 10^3 \text{ cm}^{-3} \mu\text{G}$ on the scale $l_{\text{sca}} \sim 10^{13} \text{ cm}$ and $R \sim 1 \text{ pc}$ suggest that the RM scatter and temporal scattering originate from a radio burst propagating in an inhomogeneous magneto-ionic environment near the repeating source, which may be related to a supernova remnant (SNR) or a wind nebula (PWN). For example, the observations of SNRs show that they have a magnetic field strength $B \sim$ a few μG to a few mG (47). For an SNR with the ejecta mass M_{ej} , the electron number density at R could be estimated as

$$n_e \simeq \frac{M_{\text{ej}}}{m_p (4\pi/3) R^3} = 98 \text{ cm}^{-3} \left(\frac{M_{\text{ej}}}{10 M_{\odot}} \right) \left(\frac{R}{1 \text{ pc}} \right)^{-3} \quad (\text{S11})$$

where m_p is the proton mass, and the ejecta is assumed to be dominated by hydrogen here. Thus, $\delta(n_e B_{\parallel}) \sim 10^3 \text{ cm}^{-3} \mu\text{G}$ at $R \sim 1 \text{ pc}$ is attainable for an SNR. On the other hand, according to Eq.(S6) and Eq.(S8), $l_{\text{sca}} \sim 10^{13} \text{ cm}$ is consistent with the observed temporal scattering time. In conclusion, the required parameters in Eq.(S9) are attainable for the SNR

scenario (see Refs. (9, 48) for more detailed theoretical treatments of SNR properties). At last, the DM contribution from the plasma screen is given by

$$\text{DM} \simeq n_e R = 100 \text{ pc cm}^{-3} \left(\frac{n_e}{100 \text{ cm}^{-3}} \right) \left(\frac{R}{1 \text{ pc}} \right). \quad (\text{S12})$$

This explains the large DM_{host} values observed in some of these repeating FRBs, especially FRB 20121102 (2) and FRB 20190520 (18).

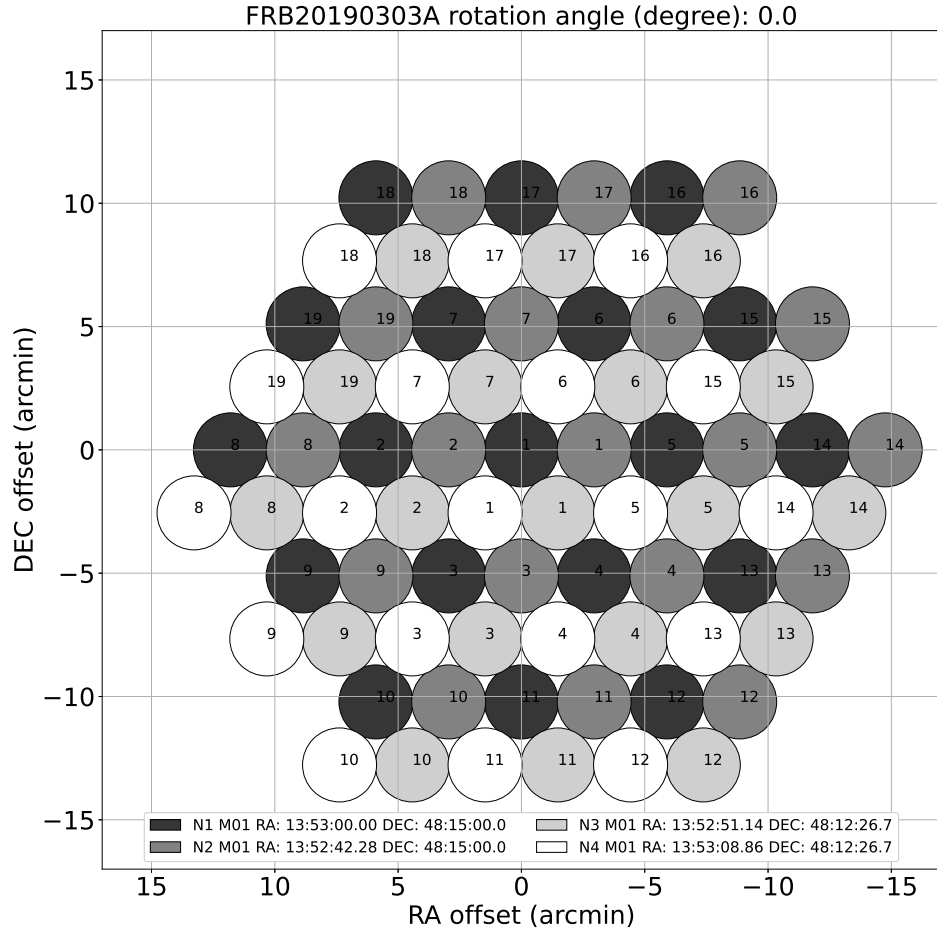
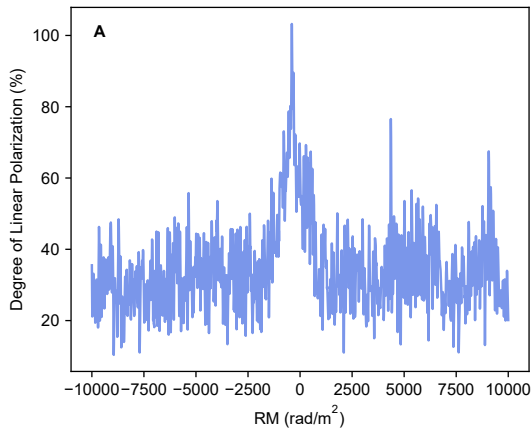
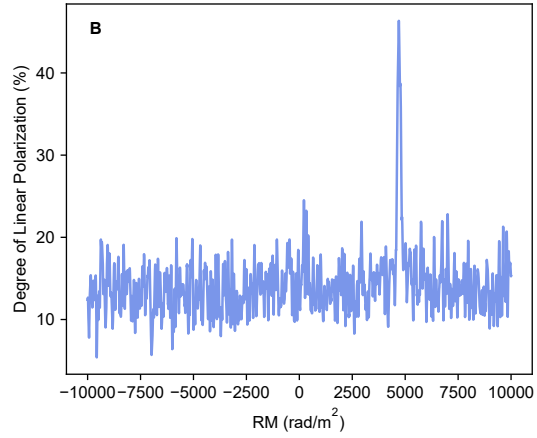


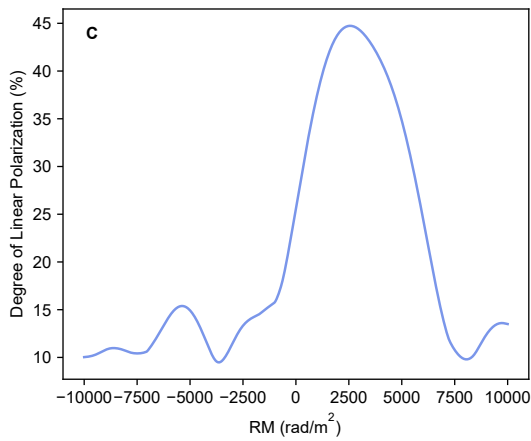
Figure S1: **Gridding observations.** Gridding observations of FRB 20190303A on 4 Jan 2021 (N1, N2) in legend and 5 Jan 2021 (N3, N4). Each pointing of N1, N2, N3 and N4 lasts for 30 minutes.



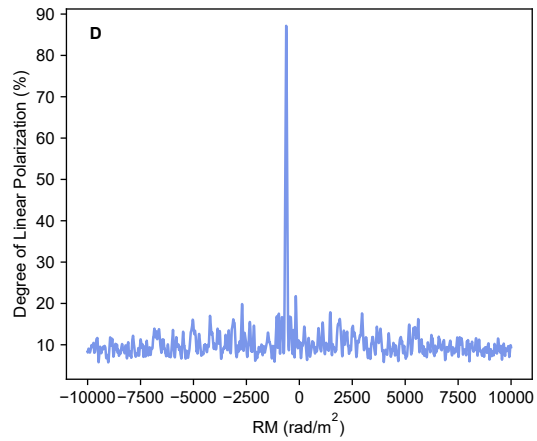
(a) FRB 20190303A



(b) FRB 20190417A



(c) FRB 20190520B



(d) FRB 20201124A

Figure S2: **RM search with RM-synthesis.** Example results of RM-synthesis for each FRB with RM detection. The blue lines represent linear polarization fraction of the bursts as a function of rotation measure.

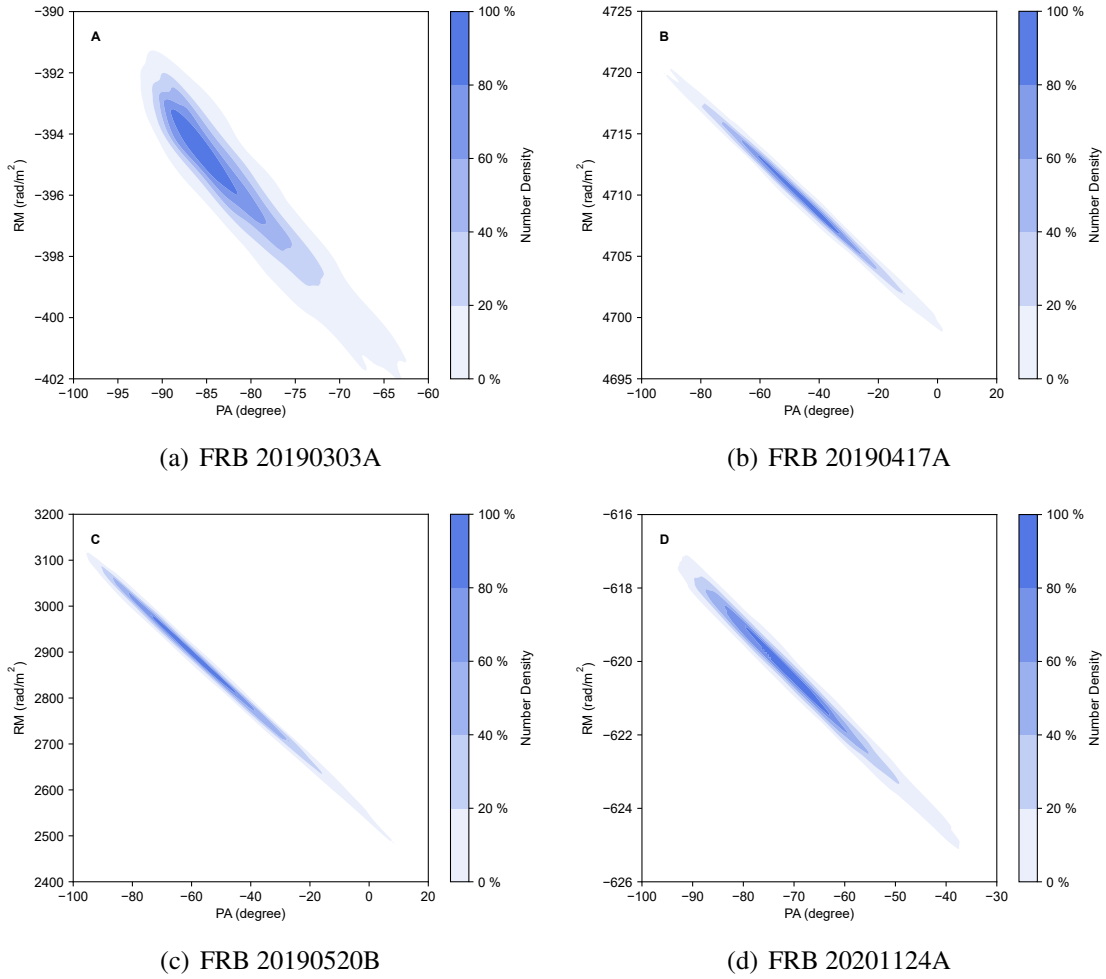
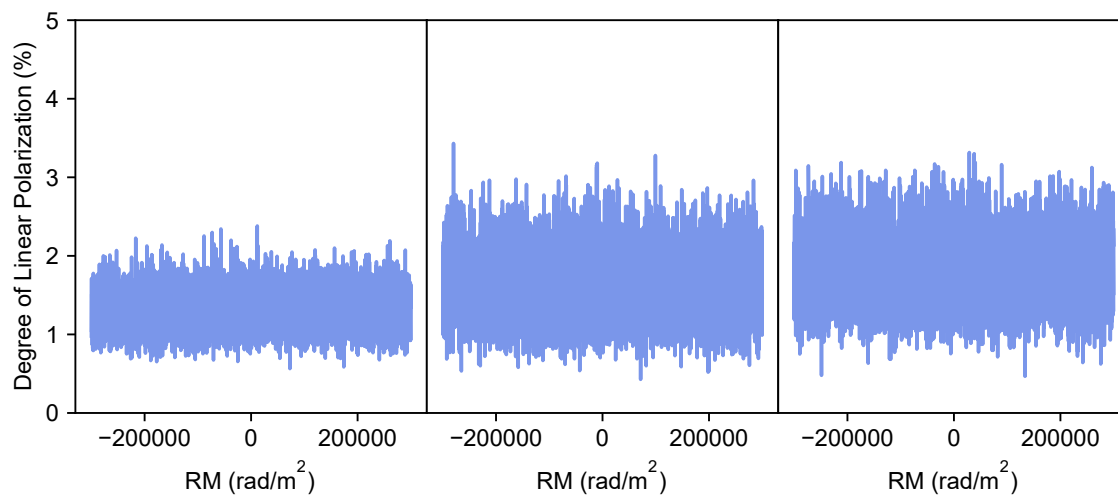
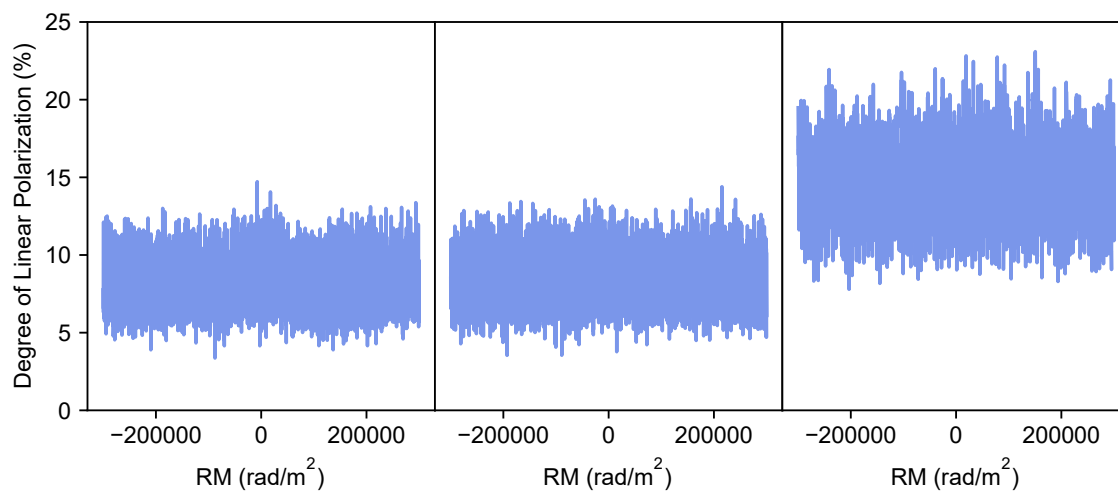


Figure S3: RM search with Stokes QU-fitting. Example results of Stokes QU-fitting for the same bursts shown in Figure S2. Each panel shows the two dimensional posterior probability distributions of the RM and PA for FRB 20190303A (Panel A), FRB 20190417A (Panel B), FRB 20190520B (Panel C) and FRB 20201124A (Panel B). The selection of contour levels is displayed in the colour bar.



(a) FRB 20121102A



(b) FRB 20190520B

Figure S4: **RM search for FRBs 20121102A and 20190520B.** RM search for the three brightest bursts of FRB 20121102A and FRB 20190520B at 1.0-1.5 GHz with FAST. No peak was found in the Faraday spectrum.

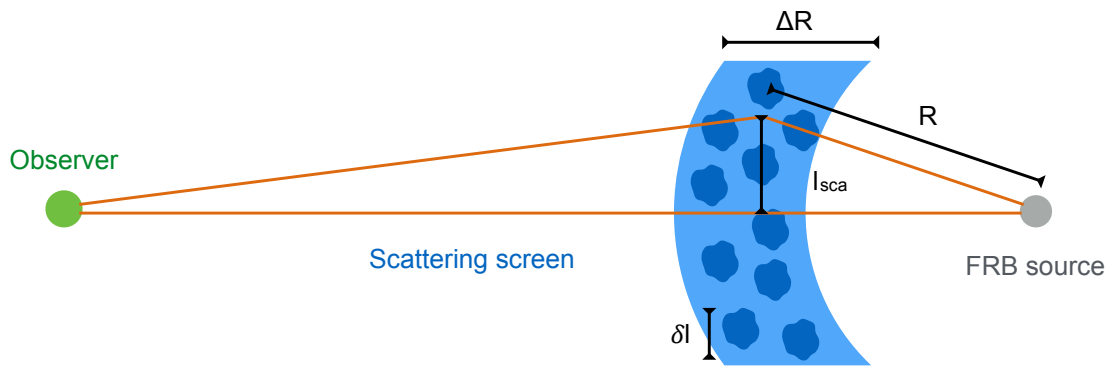


Figure S5: A **Schematic of temporal scattering and RM scatter induced by multi-path propagation.** Schematic configuration of FRB propagating in the magneto-ionic environments as the plasma screen around the FRB source.

Table S1: **Polarization properties of published FRBs.** For multiple bursts, if the bursts have nearly 100% linear polarization, we just include the brightest burst, otherwise we include each of the burst. Column (1): name of the FRB; Col.(2): Repetition; Col.(3): the telescope of the observation; Col.(4): frequency of the burst weighted by signal to noise ratio for repeaters. For non-repeaters, it is the representative frequency of the receiver; Col.(5): channel frequency width; Col.(6): fractional reduction in the linear polarization amplitude; Col.(7): rotation measure; Col.(8): degree of linear polarization; Col.(9): degree of circular polarization; Col.(10): references. ‘-’ represents not reported in the reference.

Name	Repeater	Telescope	Frequency (MHz)	$\Delta\nu$ (MHz)	f_{depol}	RM (rad m ⁻²)	% Linear	% Circular	Ref
FRB 20121102A	yes	AO	4600	1.56	7.1×10^{-3}	71525 ± 3	95.2 ± 0.4	-	(28)
		VLA	3700	0.25	9.9×10^{-4}	86550 ± 20	93 ± 2	-	(28)
		VLA	3200	0.25	2.4×10^{-3}	86550 ± 20	86 ± 1	-	(28)
FRB 20171019A	yes	GBT	820	0.10	-	-	-	-	(49)
FRB 20180301A	yes	FAST	1378	0.12	3.4×10^{-6}	$535 \pm 3^*$	85 ± 1	-	(13)
		FAST	1088	0.12	1.5×10^{-5}	548 ± 4	61 ± 4	-	(13)
		FAST	1047	0.12	1.7×10^{-5}	523 ± 9	40 ± 3	-	(13)
		FAST	1160	0.12	1.0×10^{-5}	557 ± 9	60 ± 9	-	(13)
		FAST	1094	0.12	1.5×10^{-5}	559 ± 3	70 ± 2	-	(13)
		FAST	1051	0.12	1.8×10^{-5}	549 ± 7	59 ± 5	-	(13)
		FAST	1441	0.12	2.7×10^{-6}	553 ± 13	85 ± 5	-	(13)
		FRB 20180916B	yes	CHIME	550	0.39	2.3×10^{-4}	-114.6 ± 0.6	95 ± 4
FRB 20180916B	yes	LOFAR	165	0.01	5.0×10^{-4}	-115.71 ± 0.03	70 ± 4	-	(27)
		LOFAR	155	0.01	7.4×10^{-4}	-114.78 ± 0.09	60 ± 9	-	(27)
		LOFAR	115	0.01	4.4×10^{-3}	-114.43 ± 0.04	30 ± 4	-	(27)
FRB 20190303A	yes	CHIME	600	0.39	4.5×10^{-3}	-504.4 ± 0.4	21^\dagger	-	(19)
FRB 20190604A	yes	CHIME	560	0.39	4.5×10^{-6}	-16 ± 1	100 ± 10	-	(19)
FRB 20190711A	yes	ASKAP	1220	4	1.4×10^{-6}	9 ± 2	$101 \pm 2^\ddagger$	$-1 \pm 2^\S$	(51)
FRB 20110523A	no	GBT	800	0.05	1.8×10^{-6}	-186.1 ± 1.4	44 ± 3	23 ± 30	(52)
FRB 20140514A	no	Parkes	1400	0.39	-	-	$0 \pm 10^\parallel$	21 ± 7	(53)
FRB 20150215A	no	Parkes	1400	0.39	4.4×10^{-10}	2 ± 11	43 ± 5	3 ± 1	(54)
FRB 20150418A	no	Parkes	1400	0.39	1.4×10^{-7}	$36 \pm 52^\P$	8.5 ± 1.5	0 ± 4.5	(55)
FRB 20150807A	no	Parkes	1400	0.39	1.6×10^{-8}	12 ± 1	80 ± 1	6 ± 1	(56)
FRB 20151230A	no	Parkes	1400	0.39	-	-	$35 \pm 13^\P$	6 ± 11	(57)
FRB 20160102A	no	Parkes	1400	0.39	5.3×10^{-6}	-221 ± 6	84 ± 15	30 ± 11	(57)
FRB 20180924B	no	ASKAP	1300	4	8.7×10^{-6}	22 ± 2	90.2 ± 2.0	-13.3 ± 1.4	(51)
FRB 20181112A	no	ASKAP	1300	4	2.0×10^{-6}	10.5 ± 4	$92^\#$	$-34^\#,**$	(58)
FRB 20190102C	no	ASKAP	1300	4	2.0×10^{-4}	-105 ± 1	$82.2 \pm 0.7^{\dagger\dagger}$	4.8 ± 0.5	(51)
FRB 20190608B	no	ASKAP	1300	4	2.2×10^{-3}	353 ± 2	91 ± 3	-9 ± 2	(51)
FRB 20190611B	no	ASKAP	1300	4	7.2×10^{-6}	20 ± 4	$70 \pm 3^{\dagger\dagger}$	57 ± 3	(51)

* We use value in Table 1 in Ref. (13) obtained by RM synthesis for FRB 20180301A.

[†] This is a lower bound due to possible leakage of signal of Stokes U into Stokes V. (19)

[‡] Value of sub-burst 1. Sub-burst 2 and sub-burst 3 are $94 \pm 2\%$ and $98 \pm 4\%$ linear polarized.

[§] Value of sub-burst 1. Sub-burst 2 and sub-burst 3 are $1 \pm 2\%$ and $1 \pm 3\%$ circular polarized.

^{||} RM > 118000 rad m⁻² would cause depolarization.

[¶] The linear polarization could be depolarized and the RM could be large.

[#] Value of the first pulse.

^{**} The degree of circular polarization shows a variation across the pulse, and we choose the largest absolute value of -34.

^{††} Value of sub-burst 2.

Table S2: **Properties of repeaters with σ_{RM} measurements.** Column (1): name of the FRB; Col.(2): Right Ascension (J2000); Col.(3): Declination (J2000), RAs and Decs are taken from the Transient Name Server (59); Col.(4): dispersion measure; Col.(5): rotation measure, for FRBs 20121102A, 20180301A and 20180916B, we used averaged RM in Table S1, and for the others, we used averaged RM in Table S3; Col.(6): RM scatter; Col.(7): scattering timescale, scaled to 1300 MHz assuming $\tau_{\text{sca}} \propto \lambda^4$, where λ is the wavelength. ‘-’ represents no reliable measurement.

Name	RA	Dec	DM (pc cm ⁻³)	RM (rad m ⁻²)	σ_{RM} (rad m ⁻²)	τ_{sca} ms
FRB 20121102A	05 ^h 32 ^m	+33°05′	565.8*	81542	30.9 ± 0.4	<0.43 [†]
FRB 20180301A	06 ^h 13 ^m	+04°39′	517 [‡]	546	6.3 ± 0.4	-
FRB 20180916B	01 ^h 58 ^m	+65°44′	349.2 [§]	-115	0.12 ± 0.01	0.009
FRB 20190303A	13 ^h 52 ^m	+48°07′	222.4 [¶]	-411	3.6 ± 0.1	0.19 ± 0.04 [†]
FRB 20190417A	19 ^h 39 ^m	+59°19′	1378.2 [¶]	4681	6.1 ± 0.5	0.21 ± 0.06 [†]
FRB 20190520B	16 ^h 02 ^m	-11°17′	1210.3 [#]	2759	218.9 ± 10.2	9.8 ± 2.0 [#]
FRB 20201124A	05 ^h 08 ^m	+26°03′	413.5 ^{**}	-684	2.5 ± 0.1	0.59 [†]

- * Ref (15).
- † Ref (60)
- ‡ Ref (13).
- § Ref (50).
- || Ref (27).
- ¶ Ref (19).
- # Ref (18).
- ** Ref (20).

Table S3: **Polarization Properties of FRBs.** Column (1): burst index; Col.(2): Modified Julian dates referenced to infinite frequency at the Solar System barycentre (61); Col.(3): frequency of the burst weighted by signal to noise ratio.; Col.(4): fractional reduction in the linear polarization amplitude; Col.(5): RM obtained by RM-synthesis; Col.(6): RM obtained by Stokes QU-fitting; Col.(7): degree of linear polarization; Col.(8): degree of circular polarization. ‘-’ represents not applicable.

Burst	MJD	Frequency (MHz)	f_{depol}	RM _{FDF} (rad m ⁻²)	RM _{QUfit} (rad m ⁻²)	% Linear	% Circular
FRB 20190520B (GBT 4.0-8.0 GHz, $\Delta\nu=0.37$ MHz)							
1	59292.45378759	4820	3.5×10^{-7}	2448 ± 194	2168 ⁺⁷⁵ ₋₄₉	43 ± 10	-33 ± 10
2	59296.43479679	4920	5.6×10^{-7}	3270 ± 87	3250 ⁺⁷⁷ ₋₇₁	24 ± 4	-1 ± 4
3	59300.46993279	5510	1.7×10^{-7}	2559 ± 147	2877 ⁺¹²⁶ ₋₁₅₉	43 ± 3	9 ± 3

FRB 20190303A (FAST 1.0-1.5 GHz, $\Delta\nu=0.12$ MHz)							
1	59232.95530739	1370	1.9×10^{-6}	-395 ± 14	-395_{-3}^{+2}	96 ± 16	10 ± 12
2	59258.95048596	1200	4.7×10^{-6}	-416 ± 10	-444_{-5}^{+5}	73 ± 14	3 ± 11
3	59258.96114751	1320	2.7×10^{-6}	-421 ± 11	-438_{-4}^{+7}	96 ± 11	0 ± 8
FRB 20190417A (FAST 1.0-1.5 GHz, $\Delta\nu=0.12$ MHz)							
1	59078.63698991	1128	8.8×10^{-4}	4755 ± 7	4747_{-3}^{+4}	64 ± 5	18 ± 4
2	59078.65456755	1346	2.9×10^{-4}	4652 ± 10	4655_{-2}^{+5}	86 ± 4	9 ± 3
3	59078.66719087	1125	8.4×10^{-4}	4614 ± 7	4660_{-7}^{+6}	69 ± 10	6 ± 9
4	59078.66766456	1099	9.9×10^{-4}	4671 ± 7	4670_{-5}^{+7}	76 ± 5	10 ± 4
5	59078.67199480	1075	1.2×10^{-3}	4711 ± 16	4710_{-5}^{+5}	52 ± 7	14 ± 6
FRB 20201124A (FAST 1.0-1.5 GHz, $\Delta\nu=0.12$ MHz)							
1	59316.31897656	1121	2.0×10^{-5}	-703 ± 1	-703 ± 3	97 ± 1	-6 ± 1
2	59316.33825543	1098	2.4×10^{-5}	-730 ± 1	-735 ± 4	99 ± 1	1 ± 1
3	59316.34537882	1203	1.3×10^{-5}	-710 ± 6	-709 ± 1	98 ± 1	1 ± 1
4	59316.34677951	1182	1.5×10^{-5}	-717 ± 1	-714 ± 4	95 ± 1	5 ± 1
5	59316.34798014	1302	8.0×10^{-6}	-697 ± 1	-692 ± 2	98 ± 1	-4 ± 1
6	59316.35036991	1122	2.0×10^{-5}	-701 ± 1	-703 ± 4	96 ± 1	-1 ± 1
7	59316.38275891	1059	2.7×10^{-5}	-685 ± 3	-677 ± 4	97 ± 2	-7 ± 1
8	59316.39130240	1070	2.6×10^{-5}	-696 ± 1	-700 ± 4	95 ± 1	-6 ± 1
9	59316.39532239	1107	2.1×10^{-5}	-697 ± 1	-698 ± 4	99 ± 1	-6 ± 1
10	59316.39727860	1165	1.6×10^{-5}	-710 ± 1	-707 ± 3	97 ± 1	-3 ± 1
11	59316.39841730	1250	1.0×10^{-5}	-688 ± 1	-688 ± 4	98 ± 1	-1 ± 1
FRB 20201124A (GBT 720-920 MHz, $\Delta\nu=0.20$ MHz)							
1	59315.03055957	840	2.7×10^{-4}	-665 ± 4	-662 ± 1	80 ± 3	5 ± 3
2	59315.04968094	842	2.2×10^{-4}	-603 ± 2	-603 ± 1	76 ± 3	26 ± 2
3	59315.05857900	844	3.0×10^{-4}	-707 ± 22	-702 ± 2	75 ± 3	-21 ± 2
4	59315.07106791	836	2.9×10^{-4}	-677 ± 3	-681 ± 1	75 ± 3	-6 ± 2
5	59315.07666824	839	2.4×10^{-4}	-623 ± 2	-621 ± 2	88 ± 1	-5 ± 1
6	59315.07878012	820	2.9×10^{-4}	-634 ± 1	-640 ± 1	81 ± 3	-10 ± 2
7	59315.08175219	850	2.8×10^{-4}	-698 ± 3	-701 ± 1	83 ± 2	-15 ± 2
8	59315.08311698	832	3.0×10^{-4}	-679 ± 2	-682 ± 1	78 ± 2	-2 ± 2
9	59315.08562879	844	2.7×10^{-4}	-674 ± 1	-674 ± 1	82 ± 3	-15 ± 2
FRB 20121102A (FAST 1.0-1.5 GHz, $\Delta\nu=0.12$ MHz)							
-	-	1250	2.0×10^{-1}	-	-	<6	-
FRB 20190520B (FAST 1.0-1.5 GHz, $\Delta\nu=0.12$ MHz)							
-	-	1250	1.9×10^{-4}	-	-	<20	-

References

1. D. R. Lorimer, M. Bailes, M. A. McLaughlin, D. J. Narkevic, and F. Crawford, A Bright Millisecond Radio Burst of Extragalactic Origin, *Science* **318**, 777. (2007). [10.1126/science.1147532](https://doi.org/10.1126/science.1147532)
2. L. G. Spitler, P. Scholz, J. W. T. Hessels, S. Bogdanov, A. Brazier, F. Camilo, S. Chatterjee, J. M. Cordes, F. Crawford, J. Deneva, R. D. Ferdman, P. C. C. Freire, V. M. Kaspi, P. Lazarus, R. Lynch, E. C. Madsen, M. A. McLaughlin, C. Patel, S. M. Ransom, A. Seymour, I. H. Stairs, B. W. Stappers, J. van Leeuwen, and W. W. Zhu, A repeating fast radio burst, *Nature* **531**, 202-205. (2016). [10.1038/nature17168](https://doi.org/10.1038/nature17168)
3. B. Zhang, The physical mechanisms of fast radio bursts, *Nature* **587**, 45-53. (2020). [10.1038/s41586-020-2828-1](https://doi.org/10.1038/s41586-020-2828-1)
4. B. Marcote, Z. Paragi, J. W. T. Hessels, A. Keimpema, H. J. van Langevelde, Y. Huang, C. G. Bassa, S. Bogdanov, G. C. Bower, S. Burke-Spolaor, B. J. Butler, R. M. Campbell, S. Chatterjee, J. M. Cordes, P. Demorest, M. A. Garrett, T. Ghosh, V. M. Kaspi, C. J. Law, T. J. W. Lazio, M. A. McLaughlin, S. M. Ransom, C. J. Salter, P. Scholz, A. Seymour, A. Siemion, L. G. Spitler, S. P. Tendulkar, and R. S. Wharton, The Repeating Fast Radio Burst FRB 121102 as Seen on Milliarsecond Angular Scales, *The Astrophysical Journal* **834**, L8. (2017). [10.3847/2041-8213/834/2/L8](https://doi.org/10.3847/2041-8213/834/2/L8)
5. R. Luo, K. Lee, D. R. Lorimer, and B. Zhang, On the normalized FRB luminosity function, *Monthly Notices of the Royal Astronomical Society* **481**, 2320-2337. (2018). [10.1093/mnras/sty2364](https://doi.org/10.1093/mnras/sty2364)

6. D. W. Gardenier, J. van Leeuwen, L. Connor, and E. Petroff, Synthesising the intrinsic FRB population using frbpoppy, *Astronomy and Astrophysics* **632**, A125. (2019). 10.1051/0004-6361/201936404
7. J.-P. Macquart and R. D. Ekers, Fast radio burst event rate counts - I. Interpreting the observations, *Monthly Notices of the Royal Astronomical Society* **474**, 1900-1908. (2018). 10.1093/mnras/stx2825
8. D. Michilli, A. Seymour, J. W. T. Hessels, L. G. Spitler, V. Gajjar, A. M. Archibald, G. C. Bower, S. Chatterjee, J. M. Cordes, K. Gourdji, G. H. Heald, V. M. Kaspi, C. J. Law, C. Sobey, E. A. K. Adams, C. G. Bassa, S. Bogdanov, C. Brinkman, P. Demorest, F. Fernandez, G. Hellbourg, T. J. W. Lazio, R. S. Lynch, N. Maddox, B. Marcote, M. A. McLaughlin, Z. Paragi, S. M. Ransom, P. Scholz, A. P. V. Siemion, S. P. Tendulkar, P. van Rooy, R. S. Wharton, and D. Whitlow, An extreme magneto-ionic environment associated with the fast radio burst source FRB 121102, *Nature* **553**, 182-185. (2018). 10.1038/nature25149
9. A. L. Piro and B. M. Gaensler, The Dispersion and Rotation Measure of Supernova Remnants and Magnetized Stellar Winds: Application to Fast Radio Bursts, *The Astrophysical Journal* **861**, 150. (2018). 10.3847/1538-4357/aac9bc
10. B. Margalit and B. D. Metzger, A Concordance Picture of FRB 121102 as a Flaring Magnetar Embedded in a Magnetized Ion-Electron Wind Nebula, *The Astrophysical Journal* **868**, L4. (2018). 10.3847/2041-8213/aaedad
11. W. Lu, P. Kumar, and R. Narayan, Fast radio burst source properties from polarization measurements, *Monthly Notices of the Royal Astronomical Society* **483**, 359-369. (2019). 10.1093/mnras/sty2829

12. S. Dai, J. Lu, C. Wang, W.-Y. Wang, R. Xu, Y. Yang, S. Zhang, G. Hobbs, D. Li, R. Luo, M. Filipovic, and J. Jiang, On the Circular Polarization of Repeating Fast Radio Bursts, *The Astrophysical Journal* **920**, 46. (2021). 10.3847/1538-4357/ac193d
13. R. Luo, B. J. Wang, Y. P. Men, C. F. Zhang, J. C. Jiang, H. Xu, W. Y. Wang, K. J. Lee, J. L. Han, B. Zhang, R. N. Caballero, M. Z. Chen, X. L. Chen, H. Q. Gan, Y. J. Guo, L. F. Hao, Y. X. Huang, P. Jiang, H. Li, J. Li, Z. X. Li, J. T. Luo, J. Pan, X. Pei, L. Qian, J. H. Sun, M. Wang, N. Wang, Z. G. Wen, R. X. Xu, Y. H. Xu, J. Yan, W. M. Yan, D. J. Yu, J. P. Yuan, S. B. Zhang, and Y. Zhu, Diverse polarization angle swings from a repeating fast radio burst source, *Nature* **586**, 693-696. (2020). 10.1038/s41586-020-2827-2
14. S. Chatterjee, C. J. Law, R. S. Wharton, S. Burke-Spolaor, J. W. T. Hessels, G. C. Bower, J. M. Cordes, S. P. Tendulkar, C. G. Bassa, P. Demorest, B. J. Butler, A. Seymour, P. Scholz, M. W. Abruzzo, S. Bogdanov, V. M. Kaspi, A. Keimpema, T. J. W. Lazio, B. Marcote, M. A. McLaughlin, Z. Paragi, S. M. Ransom, M. Rupen, L. G. Spitler, and H. J. van Langevelde, A direct localization of a fast radio burst and its host, *Nature* **541**, 58-61. (2017). 10.1038/nature20797
15. D. Li, P. Wang, W. W. Zhu, B. Zhang, X. X. Zhang, R. Duan, Y. K. Zhang, Y. Feng, N. Y. Tang, S. Chatterjee, J. M. Cordes, M. Cruces, S. Dai, V. Gajjar, G. Hobbs, C. Jin, M. Kramer, D. R. Lorimer, C. C. Miao, C. H. Niu, J. R. Niu, Z. C. Pan, L. Qian, L. Spitler, D. Werthimer, G. Q. Zhang, F. Y. Wang, X. Y. Xie, Y. L. Yue, L. Zhang, Q. J. Zhi, Y. Zhu, A bimodal burst energy distribution of a repeating fast radio burst source, *Nature*. **598**, 267–271 (2021). 10.1038/s41586-021-03878-5
16. The observations and data analysis are described in Materials and Methods.

17. D. Li, P. Wang, L. Qian, M. Krco, P. Jiang, Y. Yue, C. Jin, Y. Zhu, Z. Pan, R. Nan, and A. Dunning, FAST in Space: Considerations for a Multibeam, Multipurpose Survey Using China's 500-m Aperture Spherical Radio Telescope (FAST), *IEEE Microwave Magazine* **19**, 112-119. (2018). 10.1109/MMM.2018.2802178
18. C.-H. Niu, K. Aggarwal, D. Li, X. Zhang, S. Chatterjee, C.-W. Tsai, W. Yu, C. J. Law, S. Burke-Spolaor, J. M. Cordes, Y.-K. Zhang, S. Ocker, J.-M. Yao, P. Wang, Y. Feng, Y. Niino, C. Bochenek, M. Cruces, L. Connor, J.-A. Jiang, S. Dai, R. Luo, G.-D. Li, C.-C. Miao, J.-R. Niu, R. Anna-Thomas, J. Sydnor, D. Stern, W.-Y. Wang, M. Yuan, Y.-L. Yue, D.-J. Zhou, Z. Yan, W.-W. Zhu, B. Zhang, A repeating FRB in a dense environment with a compact persistent radio source, *arXiv e-prints* arXiv:2110.07418. (2021).
19. E. Fonseca, B. C. Andersen, M. Bhardwaj, P. Chawla, D. C. Good, A. Josephy, V. M. Kaspi, K. W. Masui, R. Mckinven, D. Michilli, Z. Pleunis, K. Shin, S. P. Tendulkar, K. M. Bandura, P. J. Boyle, C. Brar, T. Cassanelli, D. Cubranic, M. Dobbs, F. Q. Dong, B. M. Gaensler, G. Hinshaw, T. L. Landecker, C. Leung, D. Z. Li, H.-H. Lin, J. Mena-Parra, M. Merryfield, A. Naidu, C. Ng, C. Patel, U. Pen, M. Raffei-Ravandi, M. Rahman, S. M. Ransom, P. Scholz, K. M. Smith, I. H. Stairs, K. Vanderlinde, P. Yadav, and A. V. Zwaniga, Nine New Repeating Fast Radio Burst Sources from CHIME/FRB, *The Astrophysical Journal* **891**, L6. (2020). 10.3847/2041-8213/ab7208
20. Chime/Frb Collabortion, Recent high activity from a repeating Fast Radio Burst discovered by CHIME/FRB, *The Astronomer's Telegram* **14497**. (2021).
21. S. Johnston and M. Kerr, Polarimetry of 600 pulsars from observations at 1.4 GHz with the Parkes radio telescope, *Monthly Notices of the Royal Astronomical Society* **474**, 4629-4636. (2018). 10.1093/mnras/stx3095

22. S. A. Petrova, On the origin of orthogonal polarization modes in pulsar radio emission, *Astronomy and Astrophysics* **378**, 883-897. (2001). 10.1051/0004-6361:20011297
23. S. P. O'Sullivan, S. Brown, T. Robshaw, D. H. F. M. Schnitzeler, N. M. McClure-Griffiths, I. J. Feain, A. R. Taylor, B. M. Gaensler, T. L. Landecker, L. Harvey-Smith, and E. Carretti, Complex Faraday depth structure of active galactic nuclei as revealed by broad-band radio polarimetry, *Monthly Notices of the Royal Astronomical Society* **421**, 3300-3315. (2012). 10.1111/j.1365-2966.2012.20554.x
24. X. P. You, R. N. Manchester, W. A. Coles, G. B. Hobbs, and R. Shannon, Polarimetry of the Eclipsing Pulsar PSR J1748-2446A, *The Astrophysical Journal* **867**, 22. (2018). 10.3847/1538-4357/aadee0
25. E. J. Polzin, R. P. Breton, B. W. Stappers, B. Bhattacharyya, G. H. Janssen, S. Osłowski, M. S. E. Roberts, and C. Sobey, Long-term variability of a black widow's eclipses - A decade of PSR J2051-0827, *Monthly Notices of the Royal Astronomical Society* **490**, 889-908. (2019). 10.1093/mnras/stz2579
26. M. Xue, S. M. Ord, S. E. Tremblay, N. D. R. Bhat, C. Sobey, B. W. Meyers, S. J. McSweeney, and N. A. Swainston, MWA tied-array processing II: Polarimetric verification and analysis of two bright southern pulsars, *Publications of the Astronomical Society of Australia* **36**, e025. (2019). 10.1017/pasa.2019.19
27. Z. Pleunis, D. Michilli, C. G. Bassa, J. W. T. Hessels, A. Naidu, B. C. Andersen, P. Chawla, E. Fonseca, A. Gopinath, V. M. Kaspi, V. I. Kondratiev, D. Z. Li, M. Bhardwaj, P. J. Boyle, C. Brar, T. Cassanelli, Y. Gupta, A. Josephy, R. Karuppusamy, A. Keimpema, F. Kirsten, C. Leung, B. Marcote, K. W. Masui, R. Mckinven, B. W. Meyers, C. Ng, K. Nimmo, Z. Paragi, M. Rahman, P. Scholz, K. Shin, K. M. Smith, I. H. Stairs, and S. P. Tendulkar, LOFAR De-

- tection of 110-188 MHz Emission and Frequency-dependent Activity from FRB 20180916A, *The Astrophysical Journal* **911**, L3. (2021). 10.3847/2041-8213/abec72
28. G. H. Hilmarsson, D. Michilli, L. G. Spitler, R. S. Wharton, P. Demorest, G. Desvignes, K. Gourdji, S. Hackstein, J. W. T. Hessels, K. Nimmo, A. D. Seymour, M. Kramer, and R. Mckinven, Rotation Measure Evolution of the Repeating Fast Radio Burst Source FRB 121102, *The Astrophysical Journal* **908**, L10. (2021). 10.3847/2041-8213/abdec0
29. G. H. Hilmarsson, L. G. Spitler, R. A. Main, and D. Z. Li, Polarization properties of FRB 20201124A from detections with the Effelsberg 100-m radio telescope, *Monthly Notices of the Royal Astronomical Society* **508**, 5354-5361. (2021). 10.1093/mnras/stab2936
30. Detailed modeling and discussions can be found in supplementary text.
31. Yang, Y.-P., Q.-C. Li, and B. Zhang, Are Persistent Emission Luminosity and Rotation Measure of Fast Radio Bursts Related?, *The Astrophysical Journal* **895**, 7. (2020). 10.3847/1538-4357/ab88ab
32. R. M. Prestage, M. Bloss, J. Brandt, H. Chen, R. Creager, P. Demorest, J. Ford, G. Jones, A. Kepley, A. Kobelski, P. Marganian, M. Mello, D. McMahon, R. McCullough, J. Ray, D. A. Roshi, D. Werthimer, and M. Whitehead, The versatile GBT astronomical spectrometer (VE-GAS): Current status and future plans, *2015 URSI-USNC Radio Science Meeting 4*. (2015). 10.1109/USNC-URSI.2015.7303578
33. A. W. Hotan, W. van Straten, and R. N. Manchester, PSRCHIVE and PSRFITS: An Open Approach to Radio Pulsar Data Storage and Analysis, *Publications of the Astronomical Society of Australia* **21**, 302-309. (2004). 10.1071/AS04022
34. S. M. Ransom, New search techniques for binary pulsars, *Ph.D. Thesis* . (2001).

35. P. Jiang, Y. Yue, H. Gan, R. Yao, H. Li, G. Pan, J. Sun, D. Yu, H. Liu, N. Tang, L. Qian, J. Lu, J. Yan, B. Peng, S. Zhang, Q. Wang, Q. Li, and D. Li, Commissioning progress of the FAST, *Science China Physics, Mechanics, and Astronomy* **62**, 959502. (2019). 10.1007/s11433-018-9376-1
36. C.-H. Niu, D. Li, R. Luo, W.-Y. Wang, J. Yao, B. Zhang, W.-W. Zhu, P. Wang, H. Ye, Y.-K. Zhang, J.-. rui . Niu, N.-. yu . Tang, R. Duan, M. Krco, S. Dai, Y. Feng, C. Miao, Z. Pan, L. Qian, M. Xue, M. Yuan, Y. Yue, L. Zhang, and X. Zhang, CRAFTS for Fast Radio Bursts: Extending the Dispersion-Fluence Relation with New FRBs Detected by FAST, *The Astrophysical Journal* **909**, L8. (2021). 10.3847/2041-8213/abe7f0
37. B. R. Barsdell, M. Bailes, D. G. Barnes, and C. J. Fluke, Accelerating incoherent dedispersion, *Monthly Notices of the Royal Astronomical Society* **422**, 379-392. (2012). 10.1111/j.1365-2966.2012.20622.x
38. A. Dunning, M. Bowen, S. Castillo, Y. S. Chung, P. Doherty, D. George, D. B. Hayman, K. Jeganathan, H. Kanoniuk, S. Mackay, L. Reilly, P. Roush, S. K. W. Smart, R. D. Shaw, S. L. Smith, T. Tzioumis, V.-C. J. Venables, Design and Laboratory Testing of the Five Hundred Meter Aperture Spherical Telescope (FAST) 19 Beam L-Band Receiver *In 2017 XXXI-Ind General Assembly and Scientific Symposium of the International Union of Radio Science (URSI GASS)*, 1–4. (2017). 10.23919/URSIGASS.2017.8105012
39. S. Dai, G. Hobbs, R. N. Manchester, M. Kerr, R. M. Shannon, W. van Straten, A. Mata, M. Bailes, N. D. R. Bhat, S. Burke-Spolaor, W. A. Coles, S. Johnston, M. J. Keith, Y. Levin, S. Osłowski, D. Reardon, V. Ravi, J. M. Sarkissian, C. Tiburzi, L. Toomey, H. G. Wang, J.-B. Wang, L. Wen, R. X. Xu, W. M. Yan, and X.-J. Zhu, A study of multifrequency polarization pulse profiles of millisecond pulsars, *Monthly Notices of the Royal Astronomical Society* **449**, 3223-3262. (2015). 10.1093/mnras/stv508

40. B. J. Burn, On the depolarization of discrete radio sources by Faraday dispersion, *Monthly Notices of the Royal Astronomical Society* **133**, 67. (1966). 10.1093/mnras/133.1.67
41. M. A. Brentjens and A. G. de Bruyn, Faraday rotation measure synthesis, *Astronomy and Astrophysics* **441**, 1217-1228. (2005). 10.1051/0004-6361:20052990
42. Everett, J. E. and J. M. Weisberg, Emission Beam Geometry of Selected Pulsars Derived from Average Pulse Polarization Data, *The Astrophysical Journal* **553**, 341-357. (2001). 10.1086/320652
43. C. Sotomayor-Beltran, C. Sobey, J. W. T. Hessels, G. de Bruyn, A. Noutsos, A. Alexov, J. Anderson, A. Asgekar, I. M. Avruch, R. Beck, M. E. Bell, M. R. Bell, M. J. Bentum, G. Bernardi, P. Best, L. Birzan, A. Bonafede, F. Breitling, J. Broderick, W. N. Brouw, M. Brüggen, B. Ciardi, F. de Gasperin, R.-J. Dettmar, A. van Duin, S. Duscha, J. Eislöffel, H. Falcke, R. A. Fallows, R. Fender, C. Ferrari, W. Frieswijk, M. A. Garrett, J. Grießmeier, T. Grit, A. W. Gunst, T. E. Hassall, G. Heald, M. Hoeft, A. Horneffer, M. Iacobelli, E. Juette, A. Karastergiou, E. Keane, J. Kohler, M. Kramer, V. I. Kondratiev, L. V. E. Koopmans, M. Kuniyoshi, G. Kuper, J. van Leeuwen, P. Maat, G. Macario, S. Markoff, J. P. McKean, D. D. Mulcahy, H. Munk, E. Orru, H. Paas, M. Pandey-Pommier, M. Pilia, R. Pizzo, A. G. Polatidis, W. Reich, H. Röttgering, M. Serylak, J. Sluman, B. W. Stappers, M. Tagger, Y. Tang, C. Tasse, S. ter Veen, R. Vermeulen, R. J. van Weeren, R. A. M. J. Wijers, S. J. Wijnholds, M. W. Wise, O. Wucknitz, S. Yatawatta, and P. Zarka, Calibrating high-precision Faraday rotation measurements for LOFAR and the next generation of low-frequency radio telescopes, *Astronomy and Astrophysics* **552**, A58. (2013). 10.1051/0004-6361/201220728
44. F. Vazza, M. Brüggen, P. M. Hinz, D. Wittor, N. Locatelli, and C. Gheller, Probing the origin of extragalactic magnetic fields with Fast Radio Bursts, *Monthly Notices of the Royal Astronomical Society* **480**, 3907-3915. (2018). 10.1093/mnras/sty1968

45. N. Oppermann, H. Junklewitz, M. Greiner, T. A. Enßlin, T. Akahori, E. Carretti, B. M. Gaensler, A. Goobar, L. Harvey-Smith, M. Johnston-Hollitt, L. Pratley, D. H. F. M. Schnitzeler, J. M. Stil, and V. Vacca, Estimating extragalactic Faraday rotation, *Astronomy and Astrophysics* **575**, A118. (2015). 10.1051/0004-6361/201423995
46. P. Beniamini, P. Kumar, and R. Narayan, Faraday depolarization and induced circular polarization by multipath propagation with application to FRBs, *Monthly Notices of the Royal Astronomical Society* **510**, 4654-4668. (2022). 10.1093/mnras/stab3730
47. S. P. Reynolds, B. M. Gaensler, and F. Bocchino, Magnetic Fields in Supernova Remnants and Pulsar-Wind Nebulae, *Space Science Reviews* **166**, 231-261. (2012). 10.1007/s11214-011-9775-y
48. Yang, Y.-P. & Zhang, B., Dispersion Measure Variation of Repeating Fast Radio Burst Sources, *The Astrophysical Journal*, **847**, 22. (2017). 10.3847/1538-4357/aa8721
49. P. Kumar, R. M. Shannon, S. Osłowski, H. Qiu, S. Bhandari, W. Farah, C. Flynn, M. Kerr, D. R. Lorimer, J.-P. Macquart, C. Ng, C. J. Phillips, D. C. Price, and R. Spiewak, Faint Repetitions from a Bright Fast Radio Burst Source, *The Astrophysical Journal* **887**, L30. (2019). 10.3847/2041-8213/ab5b08
50. CHIME/FRB Collaboration, B. C. Andersen, K. Bandura, M. Bhardwaj, P. Boubel, M. M. Boyce, P. J. Boyle, C. Brar, T. Cassanelli, P. Chawla, D. Cubranic, M. Deng, M. Dobbs, M. Fandino, E. Fonseca, B. M. Gaensler, A. J. Gilbert, U. Giri, D. C. Good, M. Halpern, A. S. Hill, G. Hinshaw, C. Höfer, A. Josephy, V. M. Kaspi, R. Kothes, T. L. Landecker, D. A. Lang, D. Z. Li, H.-H. Lin, K. W. Masui, J. Mena-Parra, M. Merryfield, R. Mckinven, D. Michilli, N. Milutinovic, A. Naidu, L. B. Newburgh, C. Ng, C. Patel, U. Pen, T. Pinsonneault-Marotte, Z. Pleunis, M. Rafiei-Ravandi, M. Rahman, S. M. Ransom, A. Renard, P. Scholz, S. R. Siegel, S.

- Singh, K. M. Smith, I. H. Stairs, S. P. Tendulkar, I. Tretyakov, K. Vanderlinde, P. Yadav, and A. V. Zwaniga, CHIME/FRB Discovery of Eight New Repeating Fast Radio Burst Sources, *The Astrophysical Journal* **885**, L24. (2019). 10.3847/2041-8213/ab4a80
51. C. K. Day, A. T. Deller, R. M. Shannon, H. Qiu, K. W. Bannister, S. Bhandari, R. Ekers, C. Flynn, C. W. James, J.-P. Macquart, E. K. Mahony, C. J. Phillips, and J. Xavier Prochaska, High time resolution and polarization properties of ASKAP-localized fast radio bursts, *Monthly Notices of the Royal Astronomical Society* **497**, 3335-3350. (2020). 10.1093/mnras/staa2138
52. K. Masui, H.-H. Lin, J. Sievers, C. J. Anderson, T.-C. Chang, X. Chen, A. Ganguly, M. Jarvis, C.-Y. Kuo, Y.-C. Li, Y.-W. Liao, M. McLaughlin, U.-L. Pen, J. B. Peterson, A. Roman, P. T. Timbie, T. Voytek, and J. K. Yadav, Dense magnetized plasma associated with a fast radio burst, *Nature* **528**, 523-525. (2015). 10.1038/nature15769
53. E. Petroff, M. Bailes, E. D. Barr, B. R. Barsdell, N. D. R. Bhat, F. Bian, S. Burke-Spolaor, M. Caleb, D. Champion, P. Chandra, G. Da Costa, C. Delvaux, C. Flynn, N. Gehrels, J. Greiner, A. Jameson, S. Johnston, M. M. Kasliwal, E. F. Keane, S. Keller, J. Kocz, M. Kramer, G. Leloudas, D. Malesani, J. S. Mulchaey, C. Ng, E. O. Ofek, D. A. Perley, A. Possenti, B. P. Schmidt, Y. Shen, B. Stappers, P. Tisserand, W. van Straten, and C. Wolf, A real-time fast radio burst: polarization detection and multiwavelength follow-up, *Monthly Notices of the Royal Astronomical Society* **447**, 246-255. (2015). 10.1093/mnras/stu2419
54. E. Petroff, S. Burke-Spolaor, E. F. Keane, M. A. McLaughlin, R. Miller, I. Andreoni, M. Bailes, E. D. Barr, S. R. Bernard, S. Bhandari, N. D. R. Bhat, M. Burgay, M. Caleb, D. Champion, P. Chandra, J. Cooke, V. S. Dhillon, J. S. Farnes, L. K. Hardy, P. Jaroenjittichai, S. Johnston, M. Kasliwal, M. Kramer, S. P. Littlefair, J. P. Macquart, M. Mickaliger, A. Possenti, T. Pritchard, V. Ravi, A. Rest, A. Rowlinson, U. Sawangwit, B. Stappers, M. Sullivan, C. Tiburzi,

W. van Straten, ANTARES Collaboration, A. Albert, M. André, M. Anghinolfi, G. Anton, M. Ardid, J.-J. Aubert, T. Avgitas, B. Baret, J. Barrios-Martí, S. Basa, V. Bertin, S. Biagi, R. Bormuth, S. Bourret, M. C. Bouwhuis, R. Bruijn, J. Brunner, J. Busto, A. Capone, L. Caramete, J. Carr, S. Celli, T. Chiarusi, M. Circella, J. A. B. Coelho, A. Coleiro, R. Coniglione, H. Costantini, P. Coyle, A. Creusot, A. Deschamps, G. de Bonis, C. Distefano, I. di Palma, C. Donzaud, D. Dornic, D. Drouhin, T. Eberl, I. El Bojaddaini, D. Elsässer, A. Enzenhöfer, I. Felis, L. A. Fusco, S. Galatà, P. Gay, S. Geißelsöder, K. Geyer, V. Giordano, A. Gleixner, H. Glotin, T. Grégoire, R. Gracia-Ruiz, K. Graf, S. Hallmann, H. van Haren, A. J. Heijboer, Y. Hello, J. J. Hernández-Rey, J. Hößl, J. Hofestädt, C. Hugon, G. Illuminati, C. W. James, M. de Jong, M. Jongen, M. Kadler, O. Kalekin, U. Katz, D. Kießling, A. Kouchner, M. Kreter, I. Kreykenbohm, V. Kulikovskiy, C. Lachaud, R. Lahmann, D. Lefèvre, E. Leonora, M. Lotze, S. Loucatos, M. Marcelin, A. Margiotta, A. Marinelli, J. A. Martínez-Mora, A. Mathieu, R. Mele, K. Melis, T. Michael, P. Migliozzi, A. Moussa, C. Mueller, E. Nezri, G. E. Pāvālaš, C. Pellegrino, C. Perrina, P. Piattelli, V. Popa, T. Pradier, L. Quinn, C. Racca, G. Riccobene, K. Roensch, A. Sánchez-Losa, M. Saldaña, I. Salvadori, D. F. E. Samtleben, M. Sanguineti, P. Sapienza, J. Schnabel, T. Seitz, C. Sieger, M. Spurio, T. Stolarczyk, M. Taiuti, Y. Tayalati, A. Trovato, M. Tselengidou, D. Turpin, C. Tönnis, B. Vallage, C. Vallée, V. van Elewyck, D. Vivolo, A. Vizzoca, S. Wagner, J. Wilms, J. D. Zornoza, J. Zúñiga, H. E. S. S. Collaboration, H. Abdalla, A. Abramowski, F. Aharonian, F. Ait Benkhali, A. G. Akhperjanian, T. Andersson, E. O. Angüner, M. Arrieta, P. Aubert, M. Backes, A. Balzer, M. Barnard, Y. Becherini, J. B. Tjus, D. Berge, S. Bernhard, K. Bernlöhr, R. Blackwell, M. Böttcher, C. Boisson, J. Bolmont, P. Bordas, J. Bregeon, F. Brun, P. Brun, M. Bryan, T. Bulik, M. Capasso, S. Casanova, M. Cerruti, N. Chakraborty, R. Chalme-Calvet, R. C. G. Chaves, A. Chen, J. Chevalier, M. Chrétiens, S. Colafrancesco, G. Cologna, B. Condon, J. Conrad, Y. Cui, I. D. Davids, J. De Cock, B. Degrange, C. Deil, J. Devin, P. Dewilt, L. Dirson, A. Djannati-Ataï, W. Domainko,

A. Donath, L. O. Drury, G. Dubus, K. Dutson, J. Dyks, T. Edwards, K. Egberts, P. Eger, J.-P. Ernenwein, S. Eschbach, C. Farnier, S. Fegan, M. V. Fernandes, A. Fiasson, G. Fontaine, A. Förster, S. Funk, M. Füßling, S. Gabici, M. Gajdus, Y. A. Gallant, T. Garrigoux, G. Giavitto, B. Giebels, J. F. Glicenstein, D. Gottschall, A. Goyal, M.-H. Grondin, D. Hadasch, J. Hahn, M. Haupt, J. Hawkes, G. Heinzelmann, G. Henri, G. Hermann, O. Hervet, J. A. Hinton, W. Hofmann, C. Hoischen, M. Holler, D. Horns, A. Ivascenko, A. Jacholkowska, M. Jamrozy, M. Janiak, D. Jankowsky, F. Jankowsky, M. Jingo, T. Jogler, L. Jouvin, I. Jung-Richardt, M. A. Kastendieck, K. Katarzyński, D. Kerszberg, B. Khélifi, M. Kieffer, J. King, S. Klepser, D. Klochkov, W. Kluźniak, D. Kolitzus, N. Komin, K. Kosack, S. Krakau, M. Kraus, F. Krayzel, P. P. Krüger, H. Laffon, G. Lamanna, J. Lau, J.-P. Lees, J. Lefaucheur, V. Lefranc, A. Lemièrre, M. Lemoine-Goumard, J.-P. Lenain, E. Leser, T. Lohse, M. Lorentz, R. Liu, R. López-Coto, I. Lypova, V. Marandon, A. Marcowith, C. Mariaud, R. Marx, G. Maurin, N. Maxted, M. Mayer, P. J. Meintjes, M. Meyer, A. M. W. Mitchell, R. Moderski, M. Mohamed, L. Mohrmann, K. Morâ, E. Moulin, T. Murach, M. de Naurois, F. Niederwanger, J. Niemiec, L. Oakes, P. O'Brien, H. Odaka, S. Öttl, S. Ohm, M. Ostrowski, I. Oya, M. Padovani, M. Panter, R. D. Parsons, N. W. Pekeur, G. Pelletier, C. Perennes, P.-O. Petrucci, B. Peyaud, Q. Piel, S. Pita, H. Poon, D. Prokhorov, H. Prokoph, G. Pühlhofer, M. Punch, A. Quirrenbach, S. Raab, A. Reimer, O. Reimer, M. Renaud, R. D. L. Reyes, F. Rieger, C. Romoli, S. Rosier-Lees, G. Rowell, B. Rudak, C. B. Rulten, V. Sahakian, D. Salek, D. A. Sanchez, A. Santangelo, M. Sasaki, R. Schlickeiser, A. Schulz, F. Schüssler, U. Schwanke, S. Schwemmer, M. Settimo, A. S. Seyffert, N. Shafi, I. Shilon, R. Simoni, H. Sol, F. Spanier, G. Spengler, F. Spies, Ł. Stawarz, R. Steenkamp, C. Stegmann, F. Stinzing, K. Stycz, I. Sushch, J.-P. Tavernet, T. Tavernier, A. M. Taylor, R. Terrier, L. Tibaldo, D. Tiziani, M. Tluczykont, C. Trichard, R. Tuffs, Y. Uchiyama, D. J. V. D. Walt, C. van Eldik, C. van Rensburg, B. van Soelen, G. Vasileiadis, J. Veh, C. Venter, A. Viana, P. Vincent, J. Vink, F. Voisin, H. J. Völk, T. Vuillaume, Z. Wa-

- diasingh, S. J. Wagner, P. Wagner, R. M. Wagner, R. White, A. Wierzholska, P. Willmann, A. Wörnlein, D. Wouters, R. Yang, V. Zabalza, D. Zaborov, M. Zacharias, R. Zanin, A. A. Zdziarski, A. Zech, F. Zefi, A. Ziegler, and N. Żywucka, A polarized fast radio burst at low Galactic latitude, *Monthly Notices of the Royal Astronomical Society* **469**, 4465-4482. (2017). 10.1093/mnras/stx1098
55. E. F. Keane, S. Johnston, S. Bhandari, E. Barr, N. D. R. Bhat, M. Burgay, M. Caleb, C. Flynn, A. Jameson, M. Kramer, E. Petroff, A. Possenti, W. van Straten, M. Bailes, S. Burke-Spolaor, R. P. Eatough, B. W. Stappers, T. Totani, M. Honma, H. Furusawa, T. Hattori, T. Morokuma, Y. Niino, H. Sugai, T. Terai, N. Tominaga, S. Yamasaki, N. Yasuda, R. Allen, J. Cooke, J. Jencson, M. M. Kasliwal, D. L. Kaplan, S. J. Tingay, A. Williams, R. Wayth, P. Chandra, D. Perrodin, M. Berezina, M. Mickaliger, and C. Bassa, The host galaxy of a fast radio burst, *Nature* **530**, 453-456. (2016). 10.1038/nature17140
56. V. Ravi, R. M. Shannon, M. Bailes, K. Bannister, S. Bhandari, N. D. R. Bhat, S. Burke-Spolaor, M. Caleb, C. Flynn, A. Jameson, S. Johnston, E. F. Keane, M. Kerr, C. Tiburzi, A. V. Tuntsov, and H. K. Vedantham, The magnetic field and turbulence of the cosmic web measured using a brilliant fast radio burst, *Science* **354**, 1249-1252. (2016). 10.1126/science.aaf6807
57. M. Caleb, E. F. Keane, W. van Straten, M. Kramer, J. P. Macquart, M. Bailes, E. D. Barr, N. D. R. Bhat, S. Bhandari, M. Burgay, W. Farah, A. Jameson, F. Jankowski, S. Johnston, E. Petroff, A. Possenti, B. W. Stappers, C. Tiburzi, and V. Venkatraman Krishnan, The SURvey for Pulsars and Extragalactic Radio Bursts - III. Polarization properties of FRBs 160102 and 151230, *Monthly Notices of the Royal Astronomical Society* **478**, 2046-2055. (2018). 10.1093/mnras/sty1137

58. H. Cho, J.-P. Macquart, R. M. Shannon, A. T. Deller, I. S. Morrison, R. D. Ekers, K. W. Bannister, W. Farah, H. Qiu, M. W. Sammons, M. Bailes, S. Bhandari, C. K. Day, C. W. James, C. J. Phillips, J. X. Prochaska, and J. Tuthill, Spectropolarimetric Analysis of FRB 181112 at Microsecond Resolution: Implications for Fast Radio Burst Emission Mechanism, *The Astrophysical Journal* **891**, L38. (2020). 10.3847/2041-8213/ab7824
59. <https://www.wis-tns.org>
60. M. Amiri, B. C. Andersen, K. Bandura, S. Berger, M. Bhardwaj, M. M. Boyce, P. J. Boyle, C. Brar, D. Breitman, T. Cassanelli, P. Chawla, T. Chen, J.-F. Cliche, A. Cook, D. Cubranic, A. P. Curtin, M. Deng, M. Dobbs, F. (Adam) Dong, G. Eadie, M. Fandino, E. Fonseca, B. M. Gaensler, U. Giri, D. C. Good, M. Halpern, A. S. Hill, G. Hinshaw, A. Josephy, J. F. Kaczmarek, Z. Kader, J. W. Kania, V. M. Kaspi, T. L. Landecker, D. Lang, C. Leung, D. Li, H.-H. Lin, K. W. Masui, R. McKinven, J. Mena-Parra, M. Merryfield, B. W. Meyers, D. Michilli, N. Milutinovic, A. Mirhosseini, M. Münchmeyer, A. Naidu, L. Newburgh, C. Ng, C. Patel, U.-L. Pen, E. Petroff, T. Pinsonneault-Marotte, Z. Pleunis, M. Rafiei-Ravandi, M. Rahman, S. M. Ransom, A. Renard, P. Sanghavi, P. Scholz, J. R. Shaw, K. Shin, S. R. Siegel, A. E. Sikora, S. Singh, K. M. Smith, I. Stairs, C. M. Tan, S. P. Tendulkar, K. Vanderlinde, H. Wang, D. Wulf, A. V. Zwaniga, and CHIME/FRB Collaboration, The First CHIME/FRB Fast Radio Burst Catalog, *The Astrophysical Journal Supplement Series* **257**, 59. (2021). 10.3847/1538-4365/ac33ab
61. G. B. Hobbs, R. T. Edwards, and R. N. Manchester, TEMPO2, a new pulsar-timing package - I. An overview, *Monthly Notices of the Royal Astronomical Society* **369**, 655-672. (2006). 10.1111/j.1365-2966.2006.10302.x